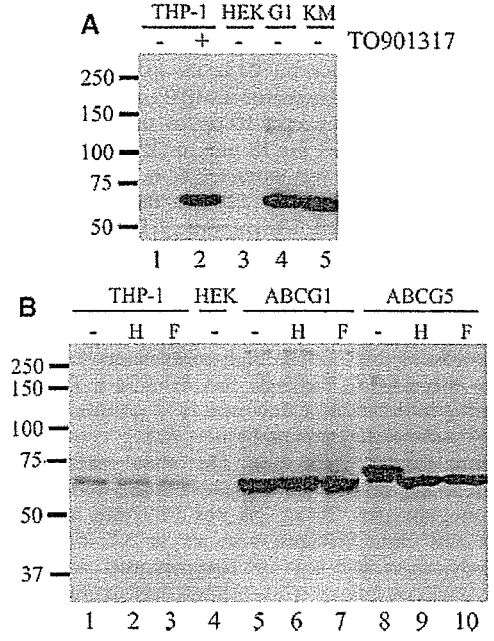


**Fig. 1.** Expression and glycosylation of ABCG1 in HEK293 and THP-1 cells. A: Cell lysates (10 μg of proteins) from THP-1 cells treated without (lane 1) or with 2.5 μM TO901317 (lane 2) or HEK293 cells (lane 3), HEK/ABCG1 cells (lane 4), or HEK/ABCG1-K120M cells (lane 5) were separated by 7% polyacrylamide gel electrophoresis. B: Membrane proteins (20 μg of proteins) from THP-1 cells treated with 1 μM TO901317 (lanes 1–3) or HEK293 cells (lane 4), HEK/ABCG1 cells (lanes 5–7), or HEK293 cells transiently expressing myc-tagged ABCG5 (lanes 8–10) were treated without (lanes 1, 4, 5, 8) or with endoglycosidase H (H; lanes 2, 6, 9) or peptide *N*-glycosidase F (F; lanes 3, 7, and 10). The samples were separated by 10% polyacrylamide gel electrophoresis. ABCG1 and ABCG5 were detected with rabbit polyclonal anti-ABCG1 or mouse monoclonal anti-myc antibody, respectively.

brane in macrophages (14, 17). However, immunostaining with anti-ABCG1 antibody suggested that the exogenously expressed ABCG1 was distributed mainly in the plasma membrane of HEK293 cells (**Fig. 2B, E**). No signal was detected in host HEK293 cells (Fig. 2A). ABCG1-K120M was also detected mainly in the plasma membrane (Fig. 2C, F), suggesting that the WalkerA lysine mutation did not affect the subcellular localization of ABCG1.

To confirm the cell surface expression of ABCG1, membrane proteins were biotinylated by sulfo-NHS-biotin and precipitated by avidin agarose (**Fig. 3**, upper panel). We also examined ABCA1 and ABCG8 as a positive and a negative control, respectively. ABCA1, which is localized mainly in the plasma membrane (20), was precipitated by avidin agarose after biotinylation (lane 2) but not without biotinylation (lane 1). On the other hand, ABCG8, which is distributed to the endoplasmic reticulum when expressed alone without ABCG5 (10), was not precipitated by avidin agarose (lane 4). ABCG1 and ABCG1-K120M were precipitated by avidin agarose after biotinylation (lanes 8, 10) but not without biotinylation (lanes 7, 9). These results indicate that ABCG1 localizes to the plasma membrane.

### Homodimerization of ABCG1

Half-type ABC proteins function as homodimers or heterodimers. ABCG2 localizes to the plasma membrane (25, 26) and functions as a homodimer (9), whereas ABCG5 and ABCG8 localize to the plasma membrane and function as heterodimers (10, 11). To examine whether ABCG1 forms a homodimer, ABCG1-myc and ABCG1-FLAG, in which each tag sequence was fused to the C terminus, were coexpressed, and immunoprecipitation was done with antibodies against tag sequences (**Fig. 4**, upper panel). When ABCG1-FLAG was immunoprecipitated with an anti-FLAG antibody, ABCG1-myc was coprecipitated (Fig. 4A, lane 4), and vice versa (Fig. 4B, lane 4). These results suggest that ABCG1 molecules interact with each other to form a homodimer or a homooligomer.

ABCG2 was reported to form a homodimer via a thiol bond (9) and to form homooligomers (27). The oligomeric features of ABCG1 were analyzed by chemical cross-linking with DSP and DTBP (**Fig. 5**). DSP and DTBP are cross-linking reagents with arm lengths of 12 and 11.9 Å, respectively, and both can be cleaved when reduced with thiols. When ABCG1 in living cells was cross-linked by DSP (lane 8) or DTBP (lane 14), ABCG1 with a molecular size of ~130 kDa was predominantly detected, which corresponds to the size of dimeric ABCG1, and was detected as a monomer when applied to SDS-PAGE after DTT treatment (lanes 11, 17). ABCG1 with higher molecular sizes was faintly detected. The electrophoretic mobility of ABCG1, without chemical cross-linking treatment on SDS-PAGE, was not altered when the sample was denatured in the absence of DTT (lane 2). ABCG1-K120M showed the same features of dimeric formation (lanes 9, 15) as the wild type. These results suggest that ABCG1 exists predominantly as a dimer without forming a thiol bond and that the WalkerA lysine mutation does not affect the dimeric formation of ABCG1.

### Binding of ATP by ABCG1

ABC proteins bind nucleotides at their NBFs and transport substrates using the energy of ATP hydrolysis. The binding of ATP by ABCG1 was analyzed using a photoaffinity labeling technique (**Fig. 6**). ABCB1 (multidrug resistance 1) was specifically photoaffinity-labeled with 8-azido-ATP as reported previously (lane 6) (28). ABCG1 was photoaffinity-labeled with 25 μM 8-azido-[α-$^{32}$P]ATP (lane 2), and the labeling was inhibited by ATP or ADP (lanes 3 and 4), demonstrating that ABCG1 can bind both ATP and ADP. The ABCG1-K120M mutant was not photoaffinity-labeled with 25 μM 8-azido-[α-$^{32}$P]ATP (lane 5), indicating that WalkerA lysine affects the nucleotide binding of ABCG1.

### Efflux of cholesterol and phospholipids by ABCG1

Because *ABCG1* mRNA expression is induced by ligands for RXR/LXR as is *ABCA1* mRNA expression (7, 14, 15), ABCG1 may be involved in cholesterol and phospholipid homeostasis in the cell. To examine the possibility that ABCG1 is involved in lipid efflux from cells as is ABCA1,

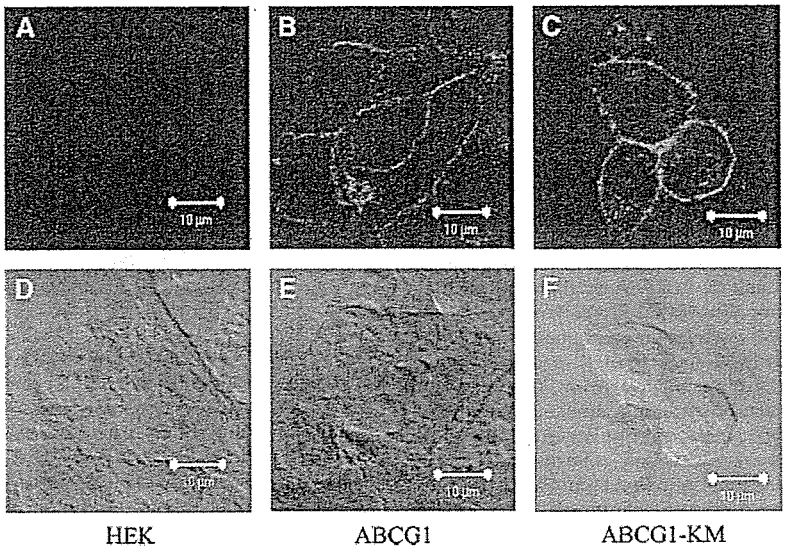


**Fig. 2.** Subcellular localization of ABCG1. HEK293 cells (A, D), HEK/ABCG1 cells (B, E), and HEK/ABCG1-K120M cells (C, F) were permeabilized with Triton X-100 and reacted with rabbit polyclonal anti-ABCG1 antibody and Alexa 488-conjugated anti-rabbit IgG. Immunostained images are shown in A–C, and differential interference contrast images are shown in D–F.

cholesterol pools of recycling endosomes were labeled with [$^3$H]cholesterol by incubating cells in DMEM containing 10% FBS and [$^3$H]cholesterol and the fractional release of [$^3$H]cholesterol to the medium after 4 h of incubation was measured (**Fig. 7A**). Host HEK293 cells did not mediate the efflux of [$^3$H]cholesterol in the absence (1.3 ± 0.41%) or presence (1.4 ± 0.41%) of apoA-I. HDL enhanced the efflux of [$^3$H]cholesterol from cells (5.6 ± 0.56%). A cell line (HEK/ABCA1) stably expressing ABCA1 mediated cholesterol efflux in the presence of apoA-I (7.3 ± 1.7%) but not in the absence of apoA-I (2.2 ± 0.45%). HEK/ABCA1 mediated slightly the higher efflux of cholesterol (7.8 ± 1.5%) than host HEK293 cells in the presence of HDL, but the difference was not significant. As reported previously (13, 19), the presence of HDL enhanced the cholesterol efflux from HEK/ABCG1 cells (11 ± 1.0%) compared with host HEK293 and HEK/ABCA1 cells. Noteworthy, HEK/ABCG1 mediated significantly higher efflux of cholesterol compared with the host HEK293 cells in the absence (3.6 ± 0.78%) or presence (4.3 ± 0.22%) of apoA-I. The release of [$^3$H]cholesterol in the absence (2.6 ± 0.74%) or presence of apoA-I (2.1 ± 0.84%) or HDL (6.8 ± 0.84%) from HEK/ABCG1-K120M cells did not significantly differ from that from host HEK293 cells. Furthermore, cells were labeled with [$^3$H]choline, and the fractional release of [$^3$H]choline phospholipids to the medium after 4 h of incubation was measured (Fig. 7B). Host HEK293 cells did not mediate the efflux of [$^3$H]choline phospholipids in the absence (0.30 ± 0.079%) or presence of apoA-I (0.23 ± 0.050%) or HDL (0.25 ± 0.080%). HEK/ABCA1 mediated phospholipid efflux in the presence of apoA-I (0.73 ± 0.15%) or HDL (0.78 ± 0.12%) but not in the absence of apoA-I (0.25 ± 0.036%). HEK/ABCG1 cells mediated higher efflux of

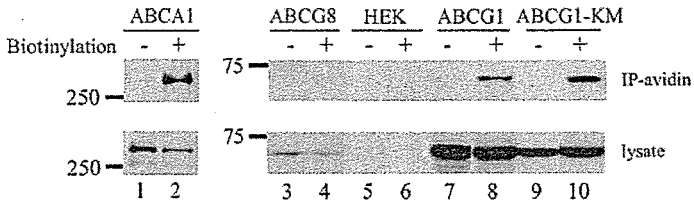


**Fig. 3.** Biotinylation of ABCG1. HEK/ABCA1 cells (lanes 1, 2), HEK/ABCG8 cells (lanes 3, 4), HEK293 cells (lanes 5, 6), HEK/ABCG1 cells (lanes 7, 8), and HEK/ABCG1-K120M cells (lanes 9, 10) were treated without (lanes 1, 3, 5, 7, 9) or with sulfo-*N*-hydroxysuccinimidobiotin (lanes 2, 4, 6, 8, and 10), and cell lysates were prepared. Biotinylated surface proteins were precipitated with avidin agarose from 100 μg of cell lysates. Cell lysates (20 μg of protein; lower panel) and precipitated surface proteins (upper panel) were separated by 10% polyacrylamide gel electrophoresis and detected with mouse monoclonal anti-ABCA1 antibody (lanes 1, 2), rabbit polyclonal anti-ABCG8 antibody (lanes 3, 4), or rabbit polyclonal anti-ABCG1 antibody (lanes 5–10). IP, immunoprecipitate.





JOURNAL OF LIPID RESEARCH

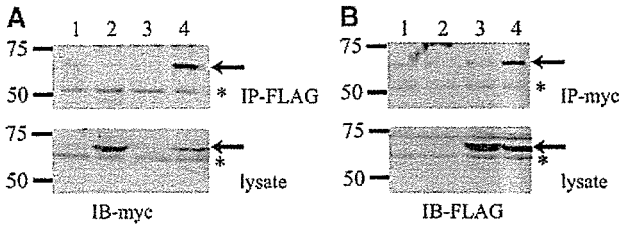


**Fig. 4.** Homomultimerization of ABCG1. HEK293 cells were transfected with mock plasmid (lane 1), ABCG1-myc (lane 2), ABCG1-FLAG (lane 3), or ABCG1-myc plus ABCG1-FLAG (lane 4), and cell lysates were prepared. ABCG1 was immunoprecipitated with rabbit polyclonal anti-FLAG antibody (A, upper panel) or mouse monoclonal anti-myc antibody (B, upper panel) from 700 μg of cell lysates. Cell lysates (20 μg of protein; lower panels) and immunoprecipitated proteins (upper panels) were separated by 10% polyacrylamide gel electrophoresis. ABCG1 was detected with mouse monoclonal anti-myc (A) or rabbit polyclonal anti-FLAG (B) antibody. Nonspecific bands are indicated by asterisks. IB, immunoblot; IP, immunoprecipitate.

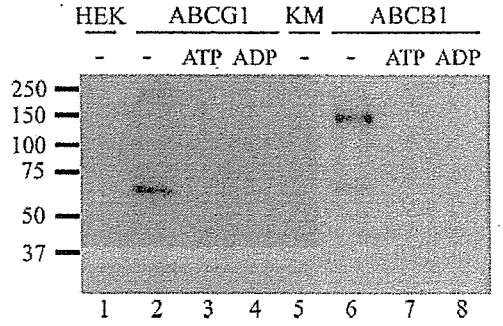


**Fig. 6.** 8-Azido-ATP binding of ABCG1. Membrane proteins (20 μg of proteins) from HEK293 cells (lane 1), HEK/ABCG1 cells (lanes 2–4), HEK/ABCG1-K120M cells (lane 5), and HEK293 cells transiently expressing ABCB1 (multidrug resistance 1) (lanes 6–8) were incubated with 25 μM 8-azido-[α-$^{32}$P]ATP in the absence (lanes 1, 2, 5, 6) or presence of 5 mM ATP (lanes 3, 7) or ADP (lanes 4, 8) for 10 min on ice followed by ultraviolet light irradiation. ABCG1 and histidine-tagged ABCB1 were immunoprecipitated with goat polyclonal anti-ABCG1 (lanes 1–5) and mouse monoclonal anti-PentaHis (lanes 6–8) antibody, respectively. Samples were separated by 10% polyacrylamide gel electrophoresis and autoradiographed.

phospholipids compared with the host HEK293 cells in the absence (0.55 ± 0.14%) or presence of apoA-I (0.58 ± 0.010%) or HDL (0.54 ± 0.014%). The release of [$^3$H]choline phospholipids in the absence (0.18 ± 0.017%) or presence of apoA-I (0.21 ± 0.023%) or HDL (0.23 ± 0.015%) from HEK/ABCG1-K120M cells did not significantly differ from that from host HEK293 cells. These results suggest that intact NBF is essential for the efflux of cholesterol and phospholipids.

Because labeling of intracellular cholesterol pools varies with methods used to deliver the labeled cholesterol or its precursors (29, 30), we further examined the efflux of cellular total cholesterol and choline phospholipids using colorimetric enzyme assays (31) (**Fig. 8**), by which we successfully measured apoA-I-dependent lipid efflux by ABCA1 and ABCA7 (32–34). The medium of host HEK293 cells contained minimal amounts of cholesterol and phospholipids. As reported previously (20), HEK/ABCA1 exhibited cholesterol and choline phospholipid efflux in an apoA-I-dependent manner. The medium of HEK/ABCG1 contained cholesterol (1.2 ± 0.025 μg/well) and choline phospholipid (0.98 ± 0.18 μg/well) at levels as high as that of HEK/ABCA1 in the presence of apoA-I (1.0 ± 0.072 and 0.84 ± 0.21 μg/well). However, surprisingly, the medium of HEK/ABCG1 contained cholesterol (0.93 ± 0.21 μg/well) and choline phospholipids (0.96 ± 0.28 μg/well) even in the absence of apoA-I. The lipid efflux by ABCA1 and ABCG1 increased in a time-dependent manner over 48 h (see supplementary Fig. I). The lipid contents were markedly reduced in the medium of HEK/ABCG1-K120M, suggesting that the binding and/or hydrolysis of ATP is required for the efflux of cholesterol and choline phospholipids by ABCG1. The intracellular contents of free cholesterol, total cholesterol, and phospholipids of HEK/ABCG1 were 15 ± 0.73, 16 ± 0.58, and 61 ± 0.50 μg/well, respectively, and not significantly different from those of HEK293 host cells. Therefore, 5.5% and 1.5% of cellular total cholesterol and phospholipids were

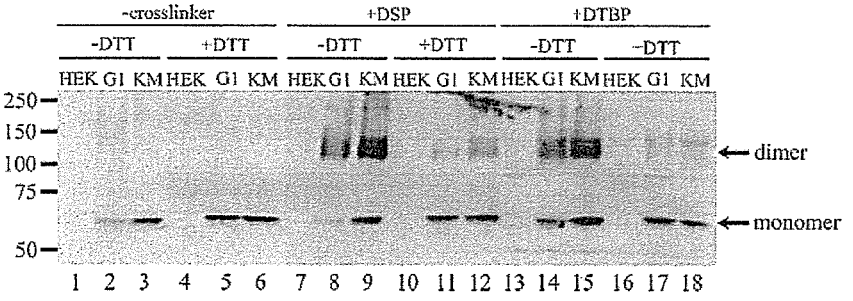


**Fig. 5.** Homodimerization of ABCG1. HEK293 cells (lanes 1, 4, 7, 10, 13, 16), HEK/ABCG1 cells (lanes 2, 5, 8, 11, 14, 17), and HEK/ABCG1-K120M cells (lanes 3, 6, 9, 12, 15, 18) were treated without (lanes 1–6) or with dithiobis (succinimidylpropionate) (DSP; lanes 7–12) or dimethyl 3,3′-dithiobispropionimidate-HCl (DTBP; lanes 13–18). Cell lysates (20 μg of protein) were treated without (lanes 1–3, 7–9, 13–15) or with DTT (lanes 4–6, 10–12, 16–18). Samples were separated by 7% polyacrylamide gel electrophoresis and detected with rabbit polyclonal anti-ABCG1 antibody.

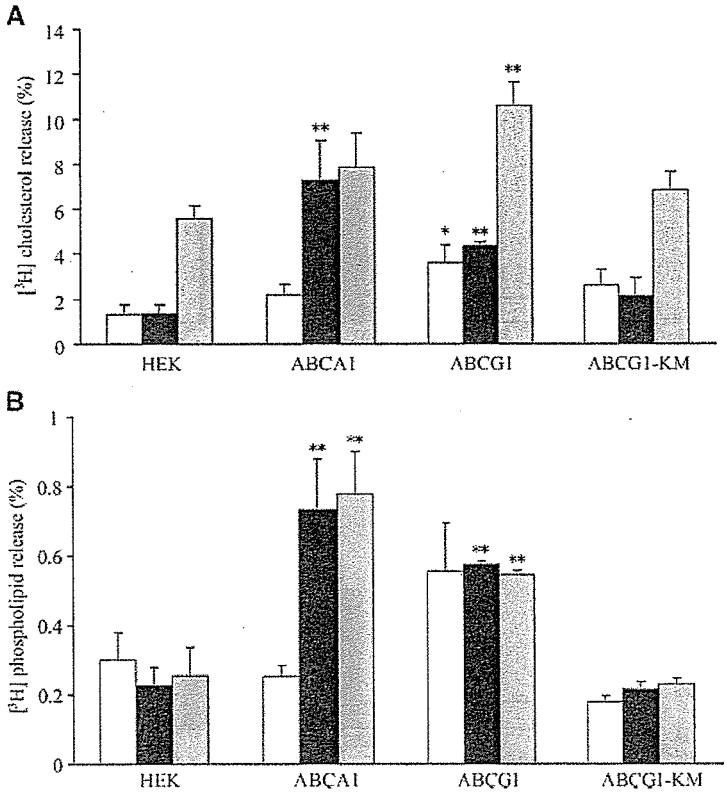


**Fig. 7.** Efflux of fractional [$^3$H]cholesterol or [$^3$H]-choline phospholipids by ABCG1. Cells were labeled with [$^3$H]cholesterol or [$^3$H]choline in DMEM containing 10% FBS for 24 h, and the efflux of [$^3$H]cholesterol (A) or [$^3$H]choline phospholipids (B) from HEK293 cells, HEK/ABCA1 cells, HEK/ABCG1 cells, or HEK/ABCG1-K120M cells during 4 h in the presence of 0.02% BSA alone (white bars), 0.02% BSA plus 10 μg/ml apolipoprotein A-I (apoA-I; black bars), or 0.02% BSA plus 20 μg/ml HDL (gray bars) was analyzed. Total [$^3$H]-choline phospholipids (cpm) in the medium were 196 ± 16 (BSA), 191 ± 50 (BSA + apoA-I), and 228 ± 77 (BSA + HDL) in HEK293 cells; 244 ± 15 (BSA), 785 ± 112 (BSA + apoA-I), and 752 ± 63 (BSA + HDL) in HEK/ABCA1 cells; 456 ± 44 (BSA), 504 ± 37 (BSA + apoA-I), and 554 ± 36 (BSA + HDL) in HEK/ABCG1 cells; and 122 ± 29 (BSA), 120 ± 14 (BSA + apoA-I), and 165 ± 8 (BSA + HDL) in HEK/ABCG1-K120M cells. Experiments were performed in triplicate, and average values are represented (±SD) as the percentage of the radioactivity in medium relative to the total radioactivity in cells and medium. * $P < 0.05$, ** $P < 0.01$ compared with host HEK293 cells.

secreted from HEK/ABCG1 in 48 h. In these experiments, expression levels of the wild-type and mutant ABCG1 were similar, and addition of apoA-I did not affect the expression (data not shown). Cell viabilities of HEK293 and HEK/ABCG1 cells [examined by 2,3-Bis(2-methoxy-4-nitro-5-sulfophenyl)-2H-tetrazolium-5-carboxanilide inner salt assay] were similar at 48 h and >98% (data not shown). To confirm that these results did not reflect a clonal bias, we examined another stable cell line of HEK/ABCG1 and found that they mediated the efflux of cholesterol and phospholipids in a similar manner (see supplementary Fig. II).

### BSA-dependent efflux of lipids by ABCG1

ABCG1 mediated the efflux of cholesterol and phospholipids even without apoA-I being added to the medium. Because the medium was supplemented with 0.02% BSA and BSA is believed to serve as a cholesterol acceptor in sperm capacitation (35), we examined the possibility that BSA works as an acceptor of cholesterol and phospholipids transported by ABCG1 (**Fig. 9A, B**). The cholesterol and phospholipid efflux by ABCG1 increased in a BSA concentration-dependent manner up to 0.02%. Surprisingly, a substantial efflux of cholesterol (0.61 ± 0.17 μg/well) and phospholipids (0.40 ± 0.023 μg/well) was observed even without BSA being added to the medium. Next, we examined whether serum proteins, including albumin, still remained in the medium after cells were washed with fresh medium: we found that significant amounts (~0.0002%) of serum albumin from FBS remained, as judged from Western blotting (see supplementary Fig. III). This suggests that serum albumin may function as an acceptor for cholesterol and phospholipids transported by ABCG1.

### Efflux of SM by ABCG1

HEK/ABCA1 and HEK/ABCG1 mediated the efflux of similar amounts of lipids with similar ratios between cholesterol and phospholipids in the presence of apoA-I, as shown in Fig. 8. The difference between the functions of ABCA1 and ABCG1 was that ABCG1 mediated the efflux even in the absence of apoA-I. We speculated that the mechanism of lipid efflux mediated by ABCG1 was different from that by ABCA1 and that phospholipid species secreted by ABCA1 and ABCG1 might be different. It has been reported that ABCA1 mediates the efflux of phospholipid, mostly PC (36). We compared the species of choline phospholipids transported by ABCA1 in the presence of apoA-I and by ABCG1 in the presence of BSA by analyzing molecular species of phospholipids in the medium with mass spectrometry (**Fig. 10**).

The media of HEK/ABCG1 cells in the presence of BSA (Fig. 10B) and HEK/ABCA1 cells in the presence of apoA-I (Fig. 10C) contained higher amounts of various choline phospholipids (SM 16:0-18:1, PC 16:0-16:1, PC 16:0-18:1, PC 18:0-18:2, and SM 24:1-18:1) than that of the host HEK293 cells in the presence of BSA (Fig. 10A). The major differences between HEK/ABCG1 and HEK/ABCA1 are

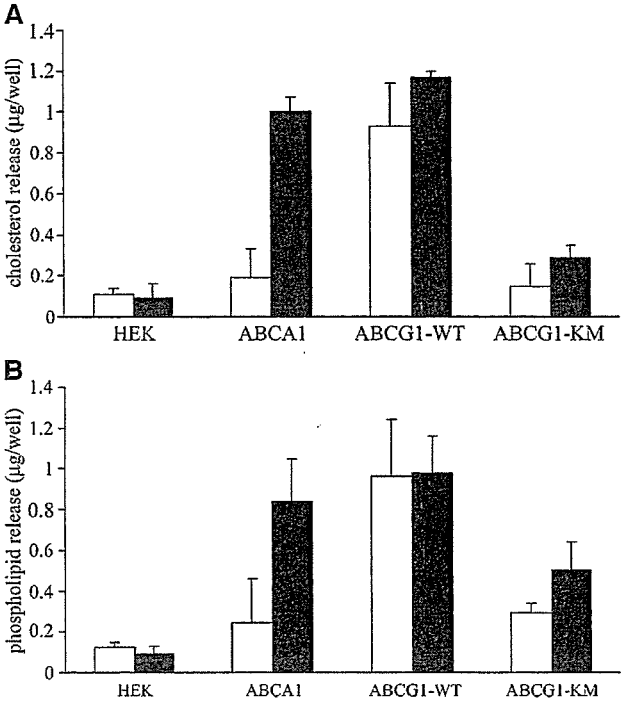


**Fig. 8.** Efflux of cellular cholesterol and phospholipids by ABCG1. The efflux of cholesterol (A) and phospholipids (B) from HEK293 cells, HEK/ABCA1 cells, HEK/ABCG1 cells, and HEK/ABCG1-K120M cells during 48 h in the presence of 0.02% BSA alone (white bars) or 0.02% BSA plus 10 μg/ml apoA-I (black bars) was analyzed. Experiments were performed in triplicate, and average values are represented (±SD).

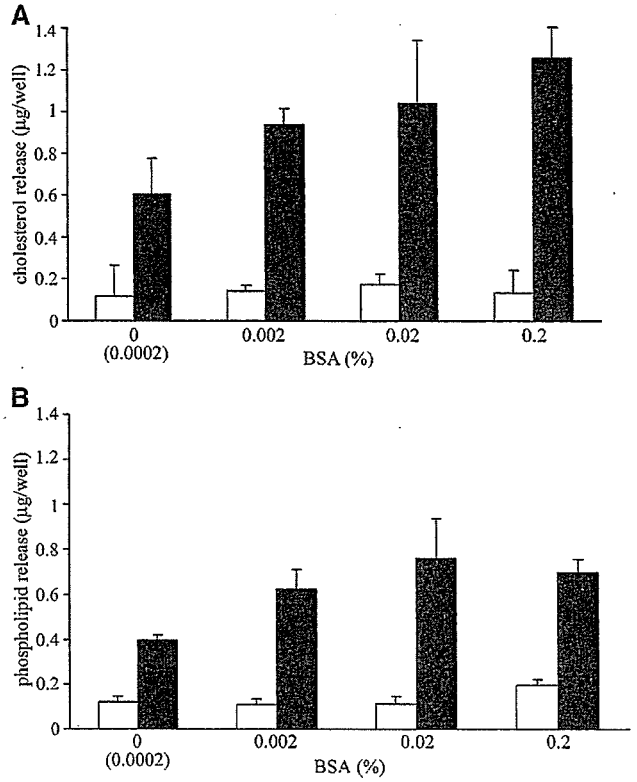


**Fig. 9.** Dependence on BSA concentration of the efflux of cholesterol and phospholipids by ABCG1. The efflux of cholesterol (A) and phospholipids (B) from HEK293 cells (white bars) or HEK/ABCG1 cells (black bars) during 24 h with the indicated concentrations of BSA was analyzed. Even in the absence of added BSA, ~0.0002% BSA was found, as judged from Western blotting against BSA, because BSA from FBS remained. Experiments were performed in triplicate, and average values are represented (±SD).

the peak heights of SM 16:0-18:1 and SM 24:1-18:1. In the medium of HEK/ABCG1 cells, the peak height of SM 16:0-18:1 was much higher than that of PC 16:0-16:1, whereas it was lower than that of PC 16:0-16:1 in the medium of HEK/ABCA1 cells. The peak height of SM 24:1-18:1 was also higher than that of PC 18:0-18:2 in the medium of HEK/ABCG1 cells, whereas it was lower than that of PC 18:0-18:2 in the medium of HEK/ABCA1 cells. Although ion peaks from a triple quadupole mass spectrometer do not allow for direct comparison between phospholipid species, the relationship between the amount of bovine brain SM and the peak height of SM 16:0-18:1 was linear from 25 to 900 μg/ml, as shown in Fig. 10C (inset). Furthermore, the relationship of the peak height of SM 16:0 was linear from 1 to 100 pmol/μl compared with 1 pmol/μl PC 16:0-16:0 (see supplementary Fig. IV). Therefore, a higher content of SM 16:0-18:1 and SM 24:1-18:1 in the medium of HEK/ABCG1 cells than in the medium of HEK/ABCA1 cells would be dependable. The medium of HEK/ABCG1 cells also included significant amounts of lysoPC 14:0, lysoPC 16:0, and lysoPC 18:1 compared with that of host HEK293 cells (data not shown), but it is not clear whether these lysoPCs were secreted from cells or converted from PC in the medium. These results suggest that ABCG1 preferentially secretes SM compared with PC, whereas ABCA1 preferentially secretes PC compared with SM.

We further examined whether ABCG1 mediated the efflux of SM (**Fig. 11**). The relative radioactivity of SM against PC secreted from HEK/ABCG1 cells in the presence of BSA (1.3 ± 0.42), apoA-I (1.1 ± 0.30), or HDL (1.3 ± 0.30) was significantly higher than that from HEK/ABCA1 in the presence of apoA-I (0.14 ± 0.045) or HDL (0.16 ± 0.012). This shows that ABCG1 mediates the efflux of SM preferentially, whereas ABCA1 mediates the efflux of PC preferentially.

## DISCUSSION

In this study, we established HEK293 cells stably expressing human ABCG1 and showed that ABCG1 localizes to the plasma membrane and mediates the efflux of cholesterol and phospholipids (preferentially SM). ABCG1 has been reported to be expressed as several splicing variants in the N-terminal region and within NBF. *ABCG1* cDNA, cloned from a fetal liver cDNA library in this study, has the same N-terminal sequence as that originally reported by Chen et al. (6). This type of variant was identified in

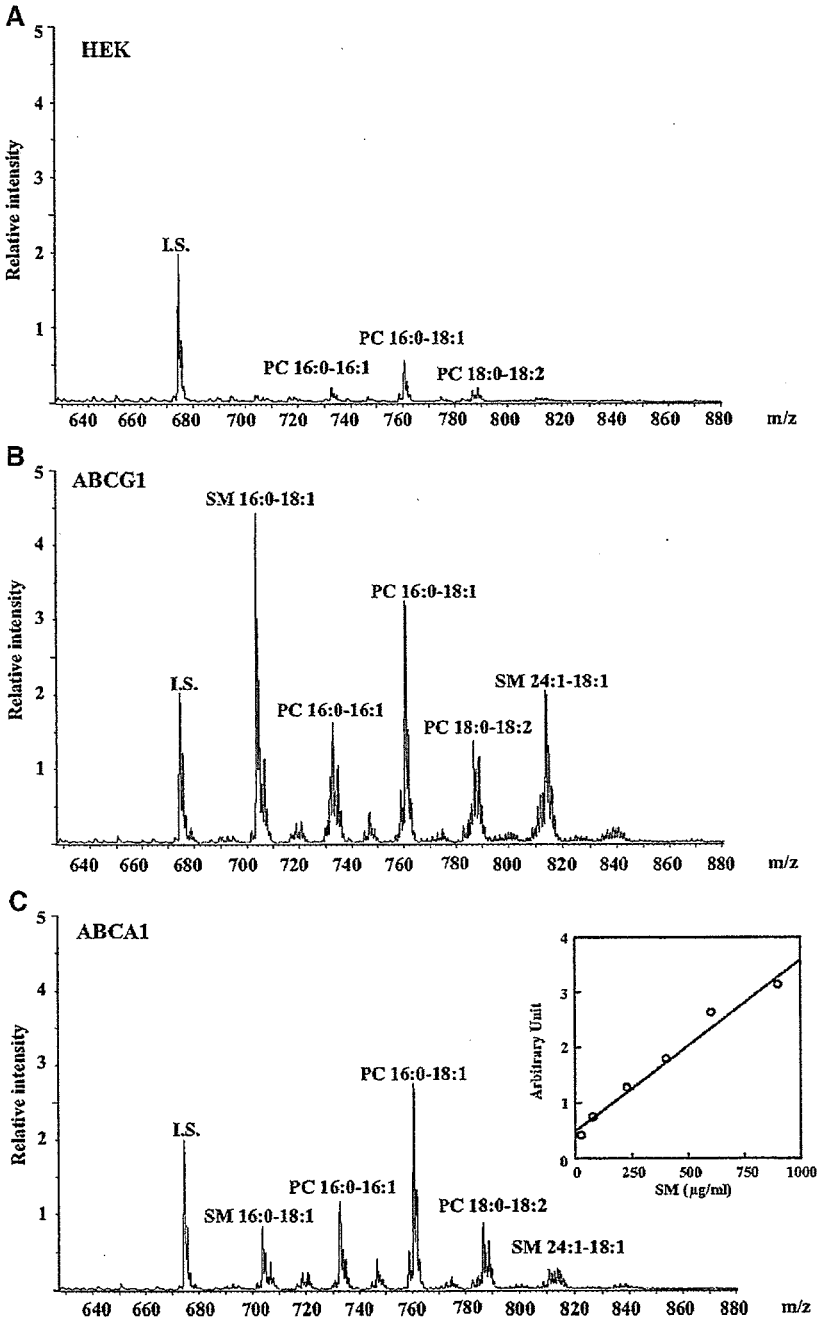


**Fig. 10.** Positive-ion electrospray ionization MS spectra of choline phospholipid molecular species in lipid extracts of the culture media. Phospholipids were extracted from the medium of HEK293 cells (A), HEK/ABCG1 cells incubated in the presence of 0.02% BSA (B), or HEK/ABCA1 cells incubated in the presence of 0.02% BSA plus 10 μg/ml apoA-I for 48 h (C). Aliquots of chloroform extracts were infused directly into the electrospray ionization ion source using an UltiMate HPLC system at a flow rate of 4 μl/min. Positive-ion electrospray ionization of lipid extracts of the cell medium was performed as described in Materials and Methods. Individual molecular species were identified using tandem mass spectrometry. The internal standard (I.S.) is 14:1-14:1 phosphatidylcholine (PC) (*m/z* 674.5) and is presented as a relative intensity value of 2. The inset in C shows the relationship between peak height and amount of sphingomyelin (SM).

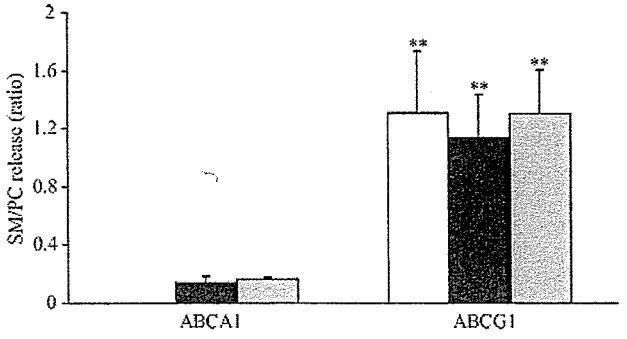


**Fig. 11.** Relative radioactivity of SM against PC. Cells were labeled with [$^3$H]choline in DMEM containing 10% FBS for 24 h, and the [$^3$H]choline phospholipids were extracted by chloroform-methanol from the medium of HEK/ABCA1 or HEK/ABCG1 cells during 4 h in the presence of 0.02% BSA alone (white bars), 0.02% BSA plus 10 μg/ml apoA-I (black bars), or 0.02% BSA plus 20 μg/ml HDL (gray bars). The extracted [$^3$H]choline phospholipids were separated by TLC, and the radioactivities of spots of PC and SM were counted. Experiments were performed in triplicate, and the relative radioactivities of SM/PC are represented (±SD). ** $P < 0.01$ compared with HEK/ABCA1 cells in the presence of apoA-I.

placenta and a macrophage cDNA library (12). The exogenously expressed ABCG1 in HEK293 cells showed a similar mobility on SDS-PAGE to the endogenous ABCG1 in THP-1 cells (Fig. 1), suggesting that the variant used in this study could be a major form in macrophages.

*N*-linked oligosaccharides are involved in the quality control of proteins by the calnexin and/or calreticulin cycle (37), and the expression of several ABC proteins has been reported to be regulated by the endoplasmic reticulum lectin (38). The isolated *ABCG1* cDNA does not contain any putative *N*-linked glycosylation sites, as reported previously in human (6) and mouse (25, 26) ABCG1, unlike that reported by Chen et al. (6). The experiment with *N*-glycosidases clearly showed that the endogenous ABCG1 in THP-1 cells is not modified by *N*-linked oligosaccharides (Fig. 1). Therefore, the major form of ABCG1 in vivo may not contain an *N*-linked glycosylation site and may function without *N*-linked oligosaccharides. It was reported that functional NBD is necessary for the trafficking of ABCG1 to the plasma membrane, because the G121A mutation within the WalkerA motif of ABCG1 abolished the cell surface expression (13). However, ABCG1-K120M localized to the plasma membrane (Fig. 2), suggesting that ATP binding and/or hydrolysis is not essential for the surface expression.

Recently, it was suggested that ABCG2 forms a multimer (27). However, cross-linking experiments show that most of the ABCG1 works as a homodimer of 60–65 kDa in an unglycosylated form, unlike ABCG2. Western blot analysis detected several bands (120–150 kDa) after cross-linking (Fig. 5). Vaughan and Oram (13) also detected similar bands by cross-linking experiment with disuccinimidyl suberate. Because we could not detect any endogenous ABCG subfamily protein (ABCG1, ABCG2, ABCG4, ABCG5, or ABCG8) in HEK293 cells by Western blot (data not shown), it is unlikely that ABCG1 forms heterodimers with endogenous ABCG subfamily proteins. ABCG1 may interact with other endogenous proteins. It was reported that ABCG1 is expressed as a protein of ~95 kDa in perinuclear structures within cholesterol-laden macrophages and is present in foamy macrophages within atherosclerotic plaques (17). It was also reported that ABCG1 is expressed on the cell surface and in intracellular compartments of cholesterol-laden macrophages as a 110 kDa protein (14). It is not clear whether the type of splicing variant and/or *N*-glycosyl modification accounts for the differences in the subcellular localization and molecular size of ABCG1 expressed in cholesterol-laden macrophages.

HEK/ABCG1 cells secrete cholesterol and choline phospholipids as efficiently as HEK/ABCA1 cells in the presence of apoA-I (Fig. 8). Because the lipid efflux by ABCG1 is impaired by the amino acid substitution of lysine in NBF, as reported for ABCA1 (39), the efflux is dependent on the function of ABCG1 operated by ATP binding and/or hydrolysis. Notably, ABCG1 mediates cholesterol and phospholipid efflux even in the absence of apoA-I, whereas lipid efflux by ABCA1 is dependent on the presence of apoA-I. Lipid efflux mediated by ABCG1 was apparently dependent on the presence of BSA (Fig. 9), suggesting that serum albumin can function as an acceptor for cholesterol and phospholipids transported by ABCG1. In the presence of 0.002% BSA, ABCG1 mediated the efflux of 0.94 μg/ml cholesterol, which suggests that the molar ratio of cholesterol and BSA is 7:1 in the medium. Phospholipids in the medium may enhance the binding of cholesterol to BSA. Alternatively, some proteins secreted from HEK293 cells may function as acceptors as well. However, even if that is the case, these molecules cannot serve as an acceptor for lipids secreted by ABCA1, suggesting that ABCG1 has broader acceptor specificity than ABCA1 has.

Recently, Cignarella et al. (40) reported cholesterol efflux from monocyte-derived macrophages in the absence of acceptors correlated with the induction of ABCG1 expression. It was also reported that ABCG1 mediates the efflux of cholesterol and phospholipids from cells to HDL-2 or HDL-3 (19). Because the expression level of ABCG1 in THP-1 cells induced by the LXR ligand was comparable to that in HEK/ABCG1 cells, direct cholesterol efflux by ABCG1 from macrophages could be important within atherosclerotic lesions, in which the amounts of lipid acceptors are limited. Furthermore, in the presence of proper acceptors of secreted cholesterol in plasma, such as HDL-2 and HDL-3, direct efflux by ABCG1 would play an important function in cholesterol and phospholipid secretion.

The mass analysis revealed that ABCG1 secretes SM as well as PC into medium from HEK/ABCG1 cells. The main constituent of the plasma membrane is PC, and it was reported that, when incubated with fibroblasts, lipid-free apoA-I produces lipoproteins containing 69% PC and 18% SM (36). Rough total peak heights of PCs in Fig. 10C can be calculated to be several fold that of

SMs. The major differences between phospholipids of HEK/ABCG1 and HEK/ABCA1 cells are the peak heights of SM 16:0-18:1 and SM 24:1-18:1. Although ion peaks from a triple quadrupole mass spectrometer do not always allow for quantitation and ion intensities of the signals are to be corrected (41), there was a linear relationship between the amount of SM and the peak height. Furthermore, the ratio of SM to PC effluxed by ABCG1 was eight times higher than that effluxed by ABCA1 (Fig. 11). From these results, it is assumed that ABCG1 preferentially secretes SM into the medium from HEK/ABCG1 cells. SM is synthesized in the lumen of the Golgi apparatus (42) and moved to the outer leaflet of the plasma membrane by vesicular membrane transport (43). SM has high affinity for cholesterol and tends to form a complex with cholesterol in the outer leaflet of the plasma membrane. ABCG1 may secrete cholesterol together with SM into the medium from the outer leaflet of the plasma membrane. It is known that the LolCDE system catalyzes the release of lipoproteins anchored to the outer leaflet of the inner membrane through the N-terminal fatty acyl chains in *Escherichia coli* (44).

In this study, we showed that the amounts of cholesterol and phospholipids in the medium of HEK/ABCG1 cells after 48 h of incubation in the presence or absence of apoA-I are similar to those of HEK/ABCA1 cells in the presence of apoA-I, as shown in Fig. 8, whereas the efficiency of cholesterol and phospholipid efflux at 4 h was not so high, as shown in Fig. 7. In a previous study, cells expressing ABCG1 showed an efflux of cholesterol to HDL-2 and HDL-3 but not to lipid-poor apoA-I (13, 19). The cause of this discrepancy is not clear, but one possible explanation is that the amounts of free cholesterol and choline phospholipids in the medium were measured by colorimetric enzyme assays in Fig. 8, whereas cells were labeled with [$^3$H]cholesterol or [$^3$H]choline and radioactivity was measured in Fig. 7 and in previous studies. Because it was reported that the labeling of intracellular cholesterol pools varies with the methods used to deliver the labeled cholesterol or its precursors (29), ABCG1 and ABCA1 might mediate the efflux of cholesterol from different intracellular pools. Another possibility may be that cells stably expressing ABCG1, at levels comparable to cells derived from human macrophages, were used in this study, whereas cells transiently expressing ABCG1 were used in the previous study. Although further studies are necessary to understand the precise mechanism of lipid efflux by ABCG1, to our knowledge, this is the first report of a protein that mediates SM efflux.

In summary, we have demonstrated that ABCG1 localizes in the plasma membrane and mediates the efflux of cholesterol and phospholipids, especially SM. ABCA1 and ABCG1 expression is coordinately induced in macrophages in the LXR pathway, and ABCA1 mediates the efflux of cholesterol and phospholipids to apolipoproteins to form preβ-HDL. In macrophages, ABCG1 may be involved in the removal of excess lipids by mediating the efflux of cholesterol and phospholipids, especially SM.

This work was supported by Grant-in-Aid for Scientific Research and Creative Scientific Research 15GS0301 from the Ministry of Education, Culture, Sports, Science, and Technology, Japan, and by grants from the Bio-oriented Technology Research Advancement Institution and the Pharmaceutical and Medical Devices Agency.

## REFERENCES

1. Takahashi, K., Y. Kimura, K. Nagata, A. Yamamoto, M. Matsuo, and K. Ueda. 2005. ABC proteins, key molecules for lipid homeostasis. *Med. Mol. Morphol.* **38:** 2–12.
2. Yu, L., J. Li-Hawkins, R. E. Hammer, K. E. Berge, J. D. Horton, J. C. Cohen, and H. H. Hobbs. 2002. Overexpression of ABCG5 and ABCG8 promotes biliary cholesterol secretion and reduces fractional absorption of dietary cholesterol. *J. Clin. Invest.* **110:** 671–680.
3. Yu, L., R. E. Hammer, J. Li-Hawkins, K. von Bergmann, D. Lutjohann, J. C. Cohen, and H. H. Hobbs. 2002. Disruption of Abcg5 and Abcg8 in mice reveals their crucial role in biliary cholesterol secretion. *Proc. Natl. Acad. Sci. USA.* **99:** 16237–16242.
4. Borst, P., N. Zelcer, and A. van Helvoort. 2000. ABC transporters in lipid transport. *Biochim. Biophys. Acta.* **1486:** 128–144.
5. Lee, J. Y., and J. S. Parks. 2005. ATP-binding cassette transporter AI and its role in HDL formation. *Curr. Opin. Lipidol.* **16:** 19–25.
6. Chen, H., C. Rossier, M. D. Lalioti, A. Lynn, A. Chakravarti, G. Perrin, and S. E. Antonarakis. 1996. Cloning of the cDNA for a human homologue of the *Drosophila* white gene and mapping to chromosome 21q22.3. *Am. J. Hum. Genet.* **59:** 66–75.
7. Kennedy, M. A., A. Venkateswaran, P. T. Tarr, I. Xenarios, J. Kudoh, N. Shimizu, and P. A. Edwards. 2001. Characterization of the human ABCG1 gene. Liver X receptor activates an internal promoter that produces a novel transcript encoding an alternative form of the protein. *J. Biol. Chem.* **276:** 39438–39447.
8. Lorkowski, S., M. Kratz, C. Wenner, R. Schmidt, B. Weitkamp, M. Fobker, J. Reinhardt, J. Rauterberg, E. A. Galinski, and P. Cullen. 2001. Expression of the ATP-binding cassette transporter gene ABCG1 (ABC8) in Tangier disease. *Biochem. Biophys. Res. Commun.* **283:** 821–830.
9. Kage, K., S. Tsukahara, T. Sugiyama, S. Asada, E. Ishikawa, T. Tsuruo, and Y. Sugimoto. 2002. Dominant-negative inhibition of breast cancer resistance protein as drug efflux pump through the inhibition of S-S dependent homodimerization. *Int. J. Cancer.* **97:** 626–630.
10. Graf, G. A., W-P. Li, R. D. Gerard, I. Gelissen, A. White, J. C. Cohen, and H. H. Hobbs. 2002. Coexpression of ATP-binding cassette proteins ABCG5 and ABCG8 permits their transport to the apical surface. *J. Clin. Invest.* **110:** 659–669.
11. Graf, G. A., L. Yu, W-P. Li, R. Gerard, P. L. Tuma, J. C. Cohen, and H. H. Hobbs. 2003. ABCG5 and ABCG8 are obligate heterodimers for protein trafficking and biliary cholesterol excretion. *J. Biol. Chem.* **278:** 48275–48282.
12. Cserepes, J., Z. Szentpetery, L. Seres, C. Ozvegy-Laczka, T. Langmann, G. Schmitz, H. Glavinas, I. Klein, L. Homolya, A. Varadi, et al. 2004. Functional expression and characterization of the human ABCG1 and ABCG4 proteins: indications for heterodimerization. *Biochem. Biophys. Res. Commun.* **320:** 860–867.
13. Vaughan, A. M., and J. F. Oram. 2005. ABCG1 redistributes cell cholesterol to domains removable by high density lipoprotein but not by lipid-depleted apolipoproteins. *J. Biol. Chem.* **280:** 30150–30157.
14. Klucken, J., C. Buchler, E. Orso, W. E. Kaminski, M. Porsch-Ozcurumez, G. Liebisch, M. Kapinsky, W. Diederich, W. Drobnik, M. Dean, et al. 2000. ABCG1 (ABC8), the human homolog of the Drosophila white gene, is a regulator of macrophage cholesterol and phospholipid transport. *Proc. Natl. Acad. Sci. USA.* **97:** 817–822.
15. Venkateswaran, A., J. J. Repa, J-M. A. Lobaccaro, A. Bronson, D. J. Mangelsdorf, and P. A. Edwards. 2000. Human white/murine ABC8 mRNA levels are highly induced in lipid-loaded macrophages. A transcriptional role for specific oxysterols. *J. Biol. Chem.* **275:** 14700–14707.
16. Hoekstra, M., J. K. Kruijt, M. Van Eck, and T. J. C. van Berkel. 2003. Specific gene expression of ATP-binding cassette transporters and

nuclear hormone receptors in rat liver parenchymal, endothelial, and Kupffer cells. *J. Biol. Chem.* **278:** 25448–25453.
17. Lorkowski, S., S. Rust, T. Engel, E. Jung, K. Tegelkamp, E. A. Galinski, G. Assmann, and P. Cullen. 2001. Genomic sequence and structure of the human ABCG1 (ABC8) gene. *Biochem. Biophys. Res. Commun.* **280:** 121–131.
18. Kennedy, M. A., G. C. Barrera, K. Nakamura, A. Baldan, P. Tarr, M. C. Fishbein, J. Frank, O. L. Francone, and P. A. Edwards. 2005. ABCG1 has a critical role in mediating cholesterol efflux to HDL and preventing cellular lipid accumulation. *Cell Metabolism.* **1:** 121–131.
19. Wang, N., D. Lan, W. Chen, F. Matsuura, and A. R. Tall. 2004. ATP-binding cassette transporters G1 and G4 mediate cellular cholesterol efflux to high-density lipoproteins. *Proc. Natl. Acad. Sci. USA.* **101:** 9774–9779.
20. Tanaka, A. R., S. Abe-Dohmae, T. Ohnishi, R. Aoki, G. Morinaga, K. I. Okuhira, Y. Ikeda, F. Kano, M. Matsuo, N. Kioka, et al. 2003. Effects of mutations of ABCA1 in the first extracellular domain on subcellular trafficking and ATP binding/hydrolysis. *J. Biol. Chem.* **278:** 8815–8819.
21. Matsuo, M., N. Kioka, T. Amachi, and K. Ueda. 1999. ATP binding properties of the nucleotide binding folds of SUR1. *J. Biol. Chem.* **274:** 37479–37482.
22. Abe-Dohmae, S., S. Suzuki, Y. Wada, H. Aburatani, D. E. Vance, and S. Yokoyama. 2000. Characterization of apolipoprotein-mediated HDL generation induced by cAMP in a murine macrophage cell line. *Biochemistry.* **39:** 11092–11099.
23. Bligh, E. C., and W. F. Dyer. 1956. A rapid method of total lipid extraction and purification. *Can. J. Biochem. Physiol.* **37:** 911–917.
24. Hiramatsu, T., H. Sonoda, Y. Takanezawa, R. Morikawa, M. Ishida, K. Kasahara, Y. Sanai, R. Taguchi, J. Aoki, and H. Arai. 2003. Biochemical and molecular characterization of two phosphatidic acid-selective phospholipase $A_1$s, mPA-PLA$_1\alpha$ and mPA-PLA$_1\beta$. *J. Biol. Chem.* **278:** 49438–49447.
25. Maliepaard, M., G. L. Scheffer, I. F. Faneyte, M. A. van Gastelen, A. C. L. M. Pijnenborg, A. H. Schinkel, M. J. van de Vijver, R. J. Scheper, and J. H. M. Schellens. 2001. Subcellular localization and distribution of the breast cancer resistance protein transporter in normal human tissues. *Cancer Res.* **61:** 3458–3464.
26. Rocchi, E., A. Khodjakov, E. L. Volk, C-H. Yang, T. Litman, S. E. Bates, and E. Schneider. 2000. The product of the ABC half-transporter gene ABCG2 (BCRP/MXR/ABCP) is expressed in the plasma membrane. *Biochem. Biophys. Res. Commun.* **271:** 42–46.
27. Xu, J., Y. Liu, Y. Yang, S. Bates, and J-T. Zhang. 2004. Characterization of oligomeric human half-ABC transporter ATP-binding cassette G2. *J. Biol. Chem.* **279:** 19781–19789.
28. Ueda, K., N. Inagaki, and S. Seino. 1997. MgADP antagonism to $Mg^{2+}$-independent ATP binding of the sulfonylurea receptor SUR1. *J. Biol. Chem.* **272:** 22983–22986.
29. Zheng, H., R. S. Kiss, V. Franklin, M-D. Wang, B. Haidar, and Y. L. Marcel. 2005. ApoA-I lipidation in primary mouse hepatocytes: separate controls for phospholipid and cholesterol transfers. *J. Biol. Chem.* **280:** 21612–21621.
30. Chen, W., Y. Sun, C. Welch, A. Gorelik, A. R. Leventhal, I. Tabas, and A. R. Tall. 2001. Preferential ATP-binding cassette transporter A1-mediated cholesterol efflux from late endosomes/lysosomes. *J. Biol. Chem.* **276:** 43564–43569.
31. Abe-Dohmae, S., S. Suzuki, Y. Wada, H. Aburatani, D. E. Vance, and S. Yokoyama. 2000. Characterization of apolipoprotein-mediated HDL generation induced by cAMP in a mouse macrophage cell line. *Biochemistry.* **39:** 11092–11099.
32. Tanaka, A. R., S. Abe-Dohmae, T. Ohnishi, R. Aoki, G. Morinaga, K-i. Okuhira, Y. Ikeda, F. Kano, M. Matsuo, N. Kioka, et al. 2003. Effects of mutations of ABCA1 in the first extracellular domain on subcellular trafficking and ATP binding/hydrolysis. *J. Biol. Chem.* **278:** 8815–8819.
33. Munehira, Y., T. Ohnishi, S. Kawamoto, A. Furuya, K. Shitara, M. Imamura, T. Yokota, S. Takeda, T. Amachi, M. Matsuo, et al. 2004. Alpha1-syntrophin modulates turnover of ABCA1. *J. Biol. Chem.* **279:** 15091–15095.
34. Abe-Dohmae, S., Y. Ikeda, M. Matsuo, M. Hayashi, K. Okuhira, K. Ueda, and S. Yokoyama. 2004. Human ABCA7 supports apolipoprotein-mediated release of cellular cholesterol and phospholipid to generate high density lipoprotein. *J. Biol. Chem.* **279:** 604–611.
35. Visconti, P. E., V. A. Westbrook, O. Chertihin, I. Demarco, S. Sleight, and A. B. Diekman. 2002. Novel signaling pathways involved in sperm acquisition of fertilizing capacity. *J. Reprod. Immunol.* **53:** 133–150.
36. Zhang, W., B. Asztalos, P. S. Roheim, and L. Wong. 1998. Characterization of phospholipids in pre-α HDL: selective phospholipid efflux with apolipoprotein A-I. *J. Lipid Res.* **39:** 1601–1607.
37. Ellgaard, L., and A. Helenius. 2003. Quality control in the endoplasmic reticulum. *Nat. Rev. Mol. Cell Biol.* **4:** 181–191.
38. Graf, G. A., J. C. Cohen, and H. H. Hobbs. 2004. Missense mutations in ABCG5 and ABCG8 disrupt heterodimerization and trafficking. *J. Biol. Chem.* **279:** 24881–24888.
39. Hamon, Y., C. Broccardo, O. Chambenoit, M. F. Luciani, F. Toti, S. Chaslin, J. M. Freyssinet, P. F. Devaux, J. McNeish, D. Marguet, et al. 2000. ABC1 promotes engulfment of apoptotic cells and transbilayer redistribution of phosphatidylserine. *Nat. Cell Biol.* **2:** 399–406.
40. Cignarella, A., T. Engel, A. von Eckardstein, M. Kratz, S. Lorkowski, A. Lueken, G. Assmann, and P. Cullen. 2005. Pharmacological regulation of cholesterol efflux in human monocyte-derived macrophages in the absence of exogenous cholesterol acceptors. *Atherosclerosis.* **179:** 229–236.
41. Brugger, B., G. Erben, R. Sandhoff, F. T. Wielandand, and W. D. Lehmann. 1997. Quantitative analysis of biological membrane lipids at the low picomole level by nano-electrospray ionization tandem mass spectrometry. *Proc. Natl. Acad. Sci. USA.* **94:** 2339–2344.
42. Huitema, K., J. van den Dikkenberg, J. F. Brouwers, and J. C. Holthuis. 2004. Identification of a family of animal sphingomyelin synthases. *EMBO J.* **23:** 33–44.
43. Burger, K. N., P. van der Bijl, and G. van Meer. 1996. Topology of sphingolipid galactosyltransferases in ER and Golgi: transbilayer movement of monohexosyl sphingolipids is required for higher glycosphingolipid biosynthesis. *J. Cell Biol.* **133:** 15–28.
44. Tokuda, H., and S-i. Matsuyama. 2004. Sorting of lipoproteins to the outer membrane in *E. coli. Biochim. Biophys. Acta.* **1693:** 5–13.

THE JOURNAL OF BIOLOGICAL CHEMISTRY VOL. 281, NO. 45, pp. 34503–34514, November 10, 2006


# Characterization and Classification of ATP-binding Cassette Transporter ABCA3 Mutants in Fatal Surfactant Deficiency*

Received for publication, January 4, 2006, and in revised form, September 5, 2006 Published, JBC Papers in Press, September 7, 2006, DOI 10.1074/jbc.M600071200

**Yoshihiro Matsumura[‡], Nobuhiro Ban[‡§], Kazumitsu Ueda[¶], and Nobuya Inagaki[‡§1]**

*From the [‡]Department of Physiology, Akita University School of Medicine, Akita 010-8543, [¶]Laboratory of Cellular Biochemistry, Division of Applied Life Sciences, Graduate School of Agriculture, Kyoto University, Kyoto 606-8502, and the [§]Department of Diabetes and Clinical Nutrition, Graduate School of Medicine, Kyoto University and CREST of Japan Science and Technology Corporation, Kyoto 606-8507, Japan*

The ATP-binding cassette transporter ABCA3 is expressed predominantly at the limiting membrane of the lamellar bodies in lung alveolar type II cells. Recent study has shown that mutation of the *ABCA3* gene causes fatal surfactant deficiency in newborns. In this study, we investigated in HEK293 cells the intracellular localization and *N*-glycosylation of the ABCA3 mutants so far identified in fatal surfactant deficiency patients. Green fluorescent protein-tagged L101P, L982P, L1553P, Q1591P, and Ins1518fs/ter1519 mutant proteins remained localized in the endoplasmic reticulum, and processing of oligosaccharide was impaired, whereas wild-type and N568D, G1221S, and L1580P mutant ABCA3 proteins trafficked to the LAMP3-positive intracellular vesicle, accompanied by processing of oligosaccharide from high mannose type to complex type. Vanadate-induced nucleotide trapping and ATP-binding analyses showed that ATP hydrolysis activity was dramatically decreased in the N568D, G1221S, and L1580P mutants, accompanied by a moderate decrease in ATP binding in N568D and L1580P mutants but not in the G1221S mutant, compared with the wild-type ABCA3 protein. In addition, mutational analyses of the Gly-1221 residue in the 11th transmembrane segment and the Leu-1580 residue in the cytoplasmic tail, and homology modeling of nucleotide binding domain 2 demonstrate the significance of these residues for ATP hydrolysis and suggest a mechanism for impaired ATP hydrolysis in G1221S and L1580P mutants. Thus, surfactant deficiency because of *ABCA3* gene mutation may be classified into two categories as follows: abnormal intracellular localization (type I) and normal intracellular localization with decreased ATP binding and/or ATP hydrolysis of the ABCA3 protein (type II). These distinct pathophysiologies may reflect both the severity and effective therapy for surfactant deficiency.

Pulmonary surfactant is a complex mixture of lipids and proteins that lowers surface tension at the air-liquid interface and prevents atelectasis (1–5). Surfactant synthesized in alveolar type II cells is stored in lamellar bodies and secreted into the alveolar space by exocytosis. The most abundant lipid in pulmonary surfactant is phosphatidylcholine, especially dipalmitoylphosphatidylcholine, and the major proteins in surfactant are surfactant protein (SP)[2]-A, SP-B, SP-C, and SP-D. In the late term of fetal lung development, several enzymes involved in lipid synthesis as well as surfactant proteins are up-regulated in preparation for adaptation to air breathing (6–9). Insufficiency of surfactant in neonates causes respiratory distress syndrome.

Three causal genes for respiratory distress syndrome identified to date are those encoding SP-B, SP-C, and ABCA3 (10–12). SP-B is an amphipathic polypeptide that is stored together with lipids in lamellar bodies and secreted into the alveoli, and its interaction with the surface of membrane is essential for the formation and maintenance of surfactant (13, 14). SP-B deficiency in infants reduces the number of lamellar bodies in alveolar type II cells, leading to lethal respiratory distress syndrome (10, 15). SP-C is a single membrane-spanning hydrophobic peptide that is stored with SP-B and lipids in lamellar bodies for secretion into alveolar space, and its insertion into the lipid membrane is thought to enhance surfactant spreading and stability (14, 16–18). Mutations in gene encoding SP-C are associated with interstitial lung disease in neonates and children (11, 20).

The function of ABCA3, a member of the A subfamily of ATP-binding cassette (ABC) transporters, is still unknown. However, because ABCA3 is expressed predominantly at the limiting membrane of the lamellar bodies in lung alveolar type II cells (21, 22), and the temporal profile and glucocorticoid responsiveness of ABCA3 expression (23) are similar to those of surfactant, we proposed that ABCA3 may be involved in surfactant secretion. Recently, Shulenin *et al.* (12) identified various *ABCA3* mutations in patients with fatal surfactant deficiency. Furthermore, very recently, *ABCA3* mutations were reported in children with interstitial lung disease (24), indicating more roles of ABCA3 in the pathophysiology of lung disease than expected. Mutations identified in patients with fatal sur-

* This work was supported by Scientific Research Grants and a Grant-in-aid for Creative Scientific Research 15GS0301 from the Ministry of Education, Culture, Sports, Science, and Technology of Japan. The costs of publication of this article were defrayed in part by the payment of page charges. This article must therefore be hereby marked "*advertisement*" in accordance with 18 U.S.C. Section 1734 solely to indicate this fact.

[1] To whom correspondence should be addressed: Dept. of Diabetes and Clinical Nutrition, Graduate School of Medicine, Kyoto University, 54 Kawahara-cho, Shogoin, Sakyo-ku, Kyoto 606-8507, Japan. Tel.: 81-75-751-3562; Fax: 81-75-771-6601; E-mail: inagaki@metab.kuhp.kyoto-u.ac.jp.

[2] The abbreviations used are: SP, surfactant protein; ABC, ATP-binding cassette; Endo H, endoglycosidase H; ER, endoplasmic reticulum; NBD, nucleotide binding domain; PNGase F, peptide *N*-glycosidase F; PNS, post-nuclear supernatant; TM, transmembrane segment; GFP, green fluorescent protein; PVDF, polyvinylidene difluoride; CFTR, cystic fibrosis transmembrane conductance regulator.

factant deficiency lie in various locations on the *ABCA3* gene (Fig. 1*A*).

In this study, to determine the pathophysiological role of these mutations in fatal surfactant deficiency, we characterized the subcellular localization, glycosylation, and ATP binding and ATP hydrolysis activities of GFP-tagged wild type and the eight ABCA3 mutants so far identified in fatal surfactant deficiency patients, expressed in cultured cells. Analyses of the ABCA3 mutants permit classification of fatal surfactant deficiency due to *ABCA3* mutation into two categories.

## EXPERIMENTAL PROCEDURES

*DNA Construction*—The coding region of human *ABCA3* cDNA without termination codon was ligated into the EcoRI and BamHI site of pEGFPN1 (Clontech) to generate pEGFPN1-ABCA3 coding ABCA3 protein fused with enhanced GFP at the C terminus. Partial cDNA fragments containing various fatal surfactant deficiency mutations (L101P, N568D, L982P, G1221S, L1553P, L1580P, Q1591P, W1142*X*, and Ins1518fs (abbreviation of Ins1518fs/ter1519 in this study), see Fig. 1*A*), were generated with PCR methods and replaced with the corresponding fragment of pEGFPN1-ABCA3. Other site-directed mutant plasmids of Gly-1221 and Leu-1580 were similarly generated. The plasmid sequences were confirmed and used for transient transfection experiments.

The coding regions of wild-type ABCA3-GFP or its mutants were inserted into the EcoRI site of pCAGIpuro, an expression vector driven by a CAG promoter (25) and containing the internal ribosomal entry site puromycin *N*-acetyltransferase gene cassette, to generate pCAGIpuro-ABCA3GFP and its mutant plasmids. These pCAGIpuro plasmid sequences were confirmed and used for stable transfection experiments.

*Confocal Microscopy*—HEK293 cells were grown at 37 °C under 5% $CO_2$ in Dulbecco's modified Eagle's medium (Sigma) supplemented with 10% fetal calf serum and penicillin/streptomycin. HEK293 cells ($3 \times 10^5$) were seeded into 35-mm dishes with poly-L-lysine-coated cover glass. After 24 h, HEK293 cells were co-transfected with wild-type or mutant pEGFP plasmid, pDsRed2-ER, and pECFP-Golgi (333 ng each) using FuGENE transfection reagent (Roche Applied Science). The transfected cells were cultured for 48 h and fixed with 4% paraformaldehyde. The cells were viewed with a Zeiss confocal microscope LSM510-META. For immunostaining of multivesicular bodies and lamellar bodies, A549 cells stably expressing ABCA3-GFP were fixed, permeabilized with 0.5% Nonidet P-40 in phosphate-buffered saline, blocked in 5% bovine serum albumin in phosphate-buffered saline, and labeled with mouse anti-human LAMP3 antibody (Chemicon) and Cy3-conjugated sheep anti-mouse IgG antibody (Amersham Biosciences). For transfection into MLE12 cells, cells were grown in Dulbecco's modified Eagle's medium/F12 medium (Invitrogen) supplemented with 2% fetal calf serum and penicillin/streptomycin and transfected using Lipofectamine 2000 reagent (Invitrogen).

*Glycosylation of ABCA3-GFP Protein and Mutants*—HEK293 cells ($3 \times 10^6$) were seeded into 100-mm dishes 24 h before transfection. Forty eight h after transfection with pEGFP vectors (6.25 μg) using FuGENE reagent, cells were homogenized in 50 mM Tris-HCl (pH 7.5) buffer containing complete protease inhibitor mixture (Roche Applied Science), by a Potter-Elvehjem homogenizer, and then centrifuged at 1,000 × *g* for 10 min to obtain post-nuclear supernatant (PNS). PNS was further centrifuged at 100,000 × *g* for 1 h to obtain the total membrane fraction. Ten μg of total membrane fraction was treated with 1 unit of peptide *N*-glycosidase F (PNGase F) or 5 milliunits of endoglycosidase H (Endo H) for 30 min at 37 °C. The deglycosylated proteins were separated by SDS-PAGE (5%) and analyzed by immunoblot analysis by using anti-GFP monoclonal antibody (Santa Cruz Biotechnology). The amount of each protein was quantified by measuring the density of the band using NIH image software, and the level of wild-type and mutant ABCA3-GFP protein in band I (Endo H-insensitive 220-kDa protein except for 190-kDa Ins1518fs protein; see Fig. 3*C*) was represented as a percentage of total band I plus band II (Endo H-sensitive 210-kDa protein except for 180-kDa Ins1518fs protein). Data are shown as means ± S.D. ($n = 3$). Statistical analysis was performed by the Bonferroni/Dunn procedure for post hoc testing.

*Establishment of HEK293 Cells and A549 Cells Stably Expressing ABCA3-GFP and Mutants*—HEK293 cells ($3 \times 10^5$) were seeded into 35-mm dishes and after 24 h were transfected with linearized wild-type pCAGIpuro-ABCA3GFP or mutant plasmid (1 μg) by PvuI using FuGENE reagent. A549 cells were grown at 37 °C under 5% $CO_2$ in RPMI 1640 medium (Sigma) supplemented with 10% fetal calf serum and penicillin/streptomycin. A549 cells ($3 \times 10^6$) were seeded into 100-mm dishes. After 24 h, cells were transfected with 6.25 μg of plasmid. Forty eight h after transfection, cells were trypsinized and seeded into 100-mm dishes and selected by 2.5 μg/ml puromycin for 7–10 days. Single colonies were isolated, and the expression of ABCA3-GFP or mutants was examined by immunoblot analysis and confocal microscopy.

*Vanadate-induced Nucleotide Trapping of ABCA3-GFP and Mutants with 8-Azido-[α-$^{32}$P]ATP*—HEK293 cells stably expressing wild-type ABCA3-GFP or mutants were disrupted in 50 mM Tris-HCl buffer (pH 7.5) containing 250 mM sucrose and complete protease inhibitor mixture by $N_2$ cavitation, followed by centrifugation at 1,000 × *g* for 10 min to obtain PNS. PNS was centrifuged at 20,000 × *g* for 30 min, and the membrane pellet was suspended in 10 mM Tris-HCl buffer (pH 7.5) containing 250 mM sucrose and 0.1 mM EGTA, and further centrifuged at 20,000 × *g* for 10 min to obtain 20,000 × *g* membrane fraction. A 20,000 × *g* membrane fraction (20–30 μg of protein) was incubated with 10 μM 8-azido-[α-$^{32}$P]ATP, 2 mM ouabain, 0.1 mM EGTA, 3 mM $MgCl_2$, and 40 mM Tris-HCl (pH 7.5) in a total volume of 12 μl for 10 min at 37 °C in the presence or absence of 0.4 mM orthovanadate, as described previously (26). The reaction was stopped by adding 400 μl of ice-cold 40 mM Tris-HCl buffer containing 0.1 mM EGTA and 1 mM $MgCl_2$. The supernatant containing unbound ATP was removed from the membrane pellet after centrifugation (20,000 × *g*, 10 min, 2 °C), and the procedure was repeated once. The pellets were resuspended in 10 μl of Tris-HCl buffer containing 0.1 mM EGTA and 1 mM $MgCl_2$ and irradiated for 10 min (at 254 nm, 8.2 milliwatts/cm$^2$) on ice. The samples were then electrophoresed on a 5% SDS-polyacryl-

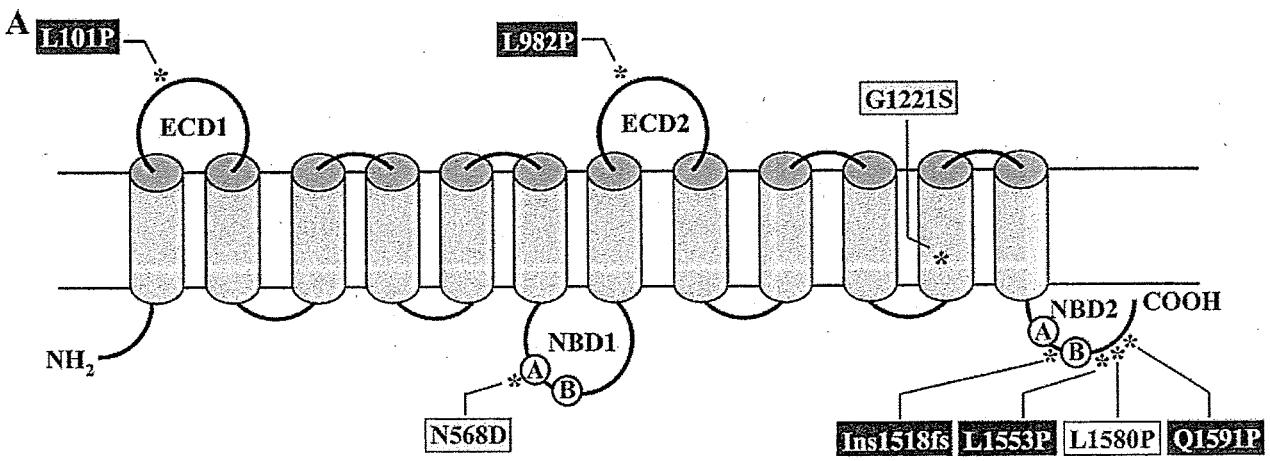


**B**

N568D WalkerA

```
hABCA3   566 GHNGAGK  571
hABCA1   933 GHNGAGK  938
hABCA2  1025 GHNGAGK 1030
hABCA4   963 GHNGAGK  968
hABCA7   841 GHNGAGK  846
hABCA12 1378 GPNGAGK 1383
             *.*****
```

**C**

G1221S

```
hABCA3   1212 RLTIFNILSGIATFLMVTIMRIP 1234
hABCA1   1769 VLTSVNLFIGINGSVATFVLELF 1791
hABCA2   1907 FLIVINLFIGITATVATFLLQLF 1929
hABCA4   1794 ALSCANLFIGINSSAITFILELF 1816
hABCA7   1650 VLTCINLFIGINGSMATFVLELF 1672
hABCA12  2101 TYVCVNLFFGIN-SIVSLSVVYF 2122
                 ... *...**. . ... ....
```

**D**

WalkerB L1553P L1580P Q1591P

```
hABCA3   1535 VIFLDEPSTGMDPVARRLLWDTVARARESGKAIIITSHSMEECEALCTRLAIMVQGQFKCLGSPQHLKSKFGSGYSLRAKV 1615
hABCA1   2065 VVFLDEPTTGMDPKARRFLWNCALSVVKEGRSVVLTSHSMEECEALCTRMAIMVNGRFRCLGSVQHLKNRFGDGYTIVVRI 2145
hABCA2   2207 FIFLDEPTTGMDPKARRFLWNLILDLIKTGRSVVLTSHSMEECEALCTRLAIMVNGRLRCLGSIQHLKNRFGDGYMITVRT 2287
hABCA4   2091 LVLLDEPTTGMDPQARRMLWNVIVSIIRKGRAVVLTSHSMEECEALCTRLAIMVKGAFRCMGTIQHLKSKFGDGYIVTMKI 2171
hABCA7   1946 VVFLDEPTTGMDPSARRFLWNSLLAVVREGRSVMLTSHSMEECEALCSRLAIMVNGRFRCLGSPQHLKGRFAAGHTLTLRV 2026
hABCA12  2410 ILLLDEPSSGMDPKSKRHLWKIISEEVQNKCSVILTSHSMEECEALCTRLAIMVNGKFQCIGSLQHIKSRFGRGFTVKVHL 2490
                .****..**** ..* **.          .... .************.*.****.* ..*.*. **.* .*. *.
```

FIGURE 1. **Structural model of ABCA3 protein and alignment of partial amino acid sequence of ABCA subfamily.** *A*, the locations of fatal surfactant deficiency mutations characterized in this study are indicated. ABCA3 is constituted by 12 putative membrane-spanning helices, two extracellular domains (*ECD*), and two nucleotide binding domains (*NBD*). *Circled A* and *B* indicate Walker A and Walker B motifs, respectively, in the two nucleotide binding domains. *Closed boxes* and *gray boxes* indicate type I and type II mutations, respectively. The Ins1518fs mutant protein lacks the C-terminal polypeptide containing the Walker B sequence of NBD-2. C-terminal amino acid sequences of wild-type and Ins1518fs mutant protein are shown. *B–D*, alignments of amino acid sequence of Walker A motif (indicated by *line*) in NBD-1 (*B*), 11th transmembrane segment (TM-11) (*C*), and partial amino acid sequence of NBD-2 including Walker B motif (indicated by *line*) (*D*) of some members of the human ABCA subfamily are shown. The amino acids residues that are conserved in six transporters and in four or five transporters are shown by *asterisks* and *dots*, respectively.

amide gel and transferred to a PVDF membrane (Millipore). The radioactivities of photoaffinity-labeled protein (total 220-kDa noncleaved form plus 180-kDa cleaved form) were quantified using FLA-5000 (Fujifilm). Radioactivities in the absence of orthovanadate were subtracted from radioactivities in the presence of orthovanadate and are represented as means ± S.D. ($n = 4$) after normalization to the ABCA3-GFP protein (total 220-kDa noncleaved form plus 180-kDa cleaved form). Statistical analysis was performed as described above.

*Binding of ABCA3-GFP and Mutants with 8-Azido-[γ-$^{32}$P]ATP*—A 20,000 × *g* membrane fraction (20–30 μg of protein) prepared as described above from HEK293 cells stably expressing wild-type ABCA3-GFP or mutants was incubated with 20 μM 8-azido-[γ-$^{32}$P]ATP, 2 mM ouabain, 0.1 mM EGTA, 3 mM $MgCl_2$, and 40 mM Tris-HCl (pH 7.5), in a total volume of 15 μl for 10 min at 0 °C (27, 28). Proteins were irradiated for 5 min (at 254 nm, 8.2 milliwatts/cm$^2$) on ice and then solubilized in RIPA buffer (50 mM Tris-HCl (pH 7.5), 150 mM NaCl, 1 mM EDTA, 1% Nonidet P-40, 0.1% SDS, and 0.5% sodium deoxycholate) containing protease inhibitor mixture for 30 min at 4 °C. After centrifugation (20,000 × *g*, 20 min, 2 °C), proteins were immunoprecipitated from the supernatant with the anti-human ABCA3 antibody (26). Samples were electrophoresed on a 5% SDS-polyacrylamide gel and transferred to a PVDF membrane. The radioactivities of photoaffinity-labeled protein (total 220-kDa noncleaved form plus 180-kDa cleaved form) were quantified using BAS-2000 (Fujifilm). To confirm the expression level of ABCA3-GFP proteins, the membrane was further analyzed by immunoblotting using anti-GFP antibody. Data normalized to the ABCA3-GFP proteins (total 220-kDa noncleaved form plus 180-kDa cleaved form) are represented as means ± S.D. ($n = 3$). Statistical analysis was performed as described above.

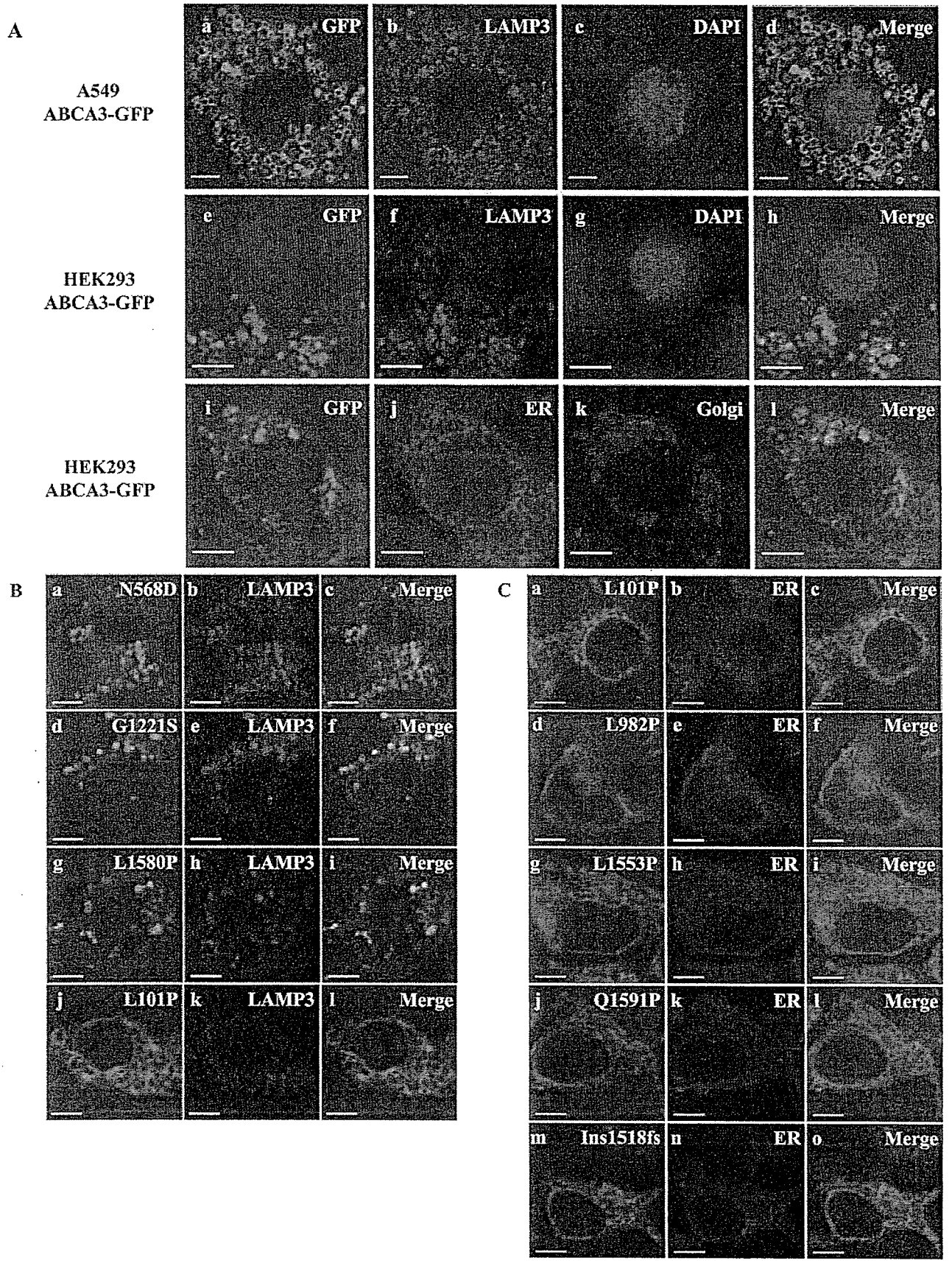

## RESULTS

*Subcellular Localization of ABCA3-GFP and Its Mutants*—We have shown previously that ABCA3 is expressed predominantly at the limiting membrane of the lamellar bodies in lung alveolar type II cells (21). Subcellular localization of ABCA3 at the intracellular vesicle membrane may be important for the function of ABCA3. When human lung adenocarcinoma A549 cells were stably transfected with pCAGIpuro-ABCA3GFP (expression plasmid for ABCA3 fused to GFP at its C terminus), most of the GFP fluorescence showed a ring-like appearance (Fig. 2*A*, *panel a*). Fluorescence signals of LAMP3, a marker of multivesicular bodies or lamellar bodies (29, 30), were mainly detected at GFP fluorescence-positive vesicles (Fig. 2*A*, *panels b* and *d*), indicating that ABCA3-GFP mainly localizes at the limiting membrane of multivesicular bodies or lamellar bodies in A549 cells. Next, HEK293 cells were transiently transfected with pEGFPN1-ABCA3. Most of the GFP fluorescence was located at dot-like vesicles (Fig. 2*A*, *panel e*), and fluorescence signals of LAMP3 were mainly detected at the GFP fluorescence-positive vesicles (*panels f* and *h*) as in A549 cells. The HEK293 cells then were co-transfected with pEGFPN1-ABCA3, pDsRed2-ER, and pECFP-Golgi plasmids for fluorescent labeling of ABCA3, the endoplasmic reticulum (ER), and the Golgi apparatus, respectively. Most of the GFP fluorescence showed a dot-like appearance (Fig. 2*A*, *panel i*), and a few signals of GFP fluorescence were merged with DsRed2 fluorescence of the ER and cyan fluorescent protein fluorescence of the Golgi apparatus (Fig. 2*A*, *panels j–l*). These results indicate that ABCA3-GFP is mainly localized at the LAMP3-positive intracellular vesicle membrane in HEK293 cells, mimicking the sorting of ABCA3-GFP in alveolar type II cells and A549 cells.

To examine the effect of the mutations found in fatal surfactant deficiency patients on subcellular localization of ABCA3, wild-type and mutant ABCA3-GFP (seven missense mutations L101P, N568D, L982P, G1221S, L1553P, L1580P, and Q1591P, and one nonsense mutation, Ins1518fs) were transiently expressed in HEK293 cells (Fig. 1*A*). The N568D, G1221S, and L1580P mutant proteins were mainly localized to the LAMP3-positive intracellular vesicle membrane (Fig. 2*B*, *panels a–c*, *d–f*, and *g–i*), similar to wild-type ABCA3 protein (Fig. 2*A*, *panels e–h*). In contrast, the L101P, L982P, L1553P, Q1591P, and Ins1518fs mutant proteins were barely detectable at the LAMP3-positive intracellular vesicle membrane (Fig. 2*B panels j–l* for L101P and data not shown for others). The GFP fluorescence of these mutant proteins was merged with the DsRed2 fluorescence of the ER (Fig. 2*C*), suggesting that these mutant proteins are mainly localized at the ER. In another cell line, mouse lung epithelial MLE12 cells, transiently expressed GFP-tagged wild-type and N568D, G1221S, and L1580P mutant proteins were mainly localized at the intracellular vesicle membrane, whereas the L101P, L982P, L1553P, Q1591P, and Ins1518fs mutant proteins were mainly localized to the ER (data not shown), confirming defective intracellular sorting of L101P, L982P, L1553P, Q1591P, and Ins1518fs ABCA3 mutant proteins.

*Glycosylation and Processing of ABCA3-GFP and Mutants*—To examine the relationship between subcellular localization and *N*-glycosylation of ABCA3 proteins, the total membrane fraction from transiently transfected HEK293 cells was analyzed by immunoblotting using anti-GFP antibody. Two bands at about 220 kDa (noncleaved form) and 180 kDa (cleaved form) (Fig. 3*A*) were detected in the wild-type ABCA3-GFP protein, consistent with our previous report that both the 190-kDa noncleaved form and the 150-kDa cleaved form were detected when human ABCA3 without the GFP tag was overexpressed in HEK293 cells (26). In the N568D, G1221S, and L1580P mutant proteins, which were mainly localized to the intracellular vesicle membrane, both the 220-kDa noncleaved form and the 180-kDa cleaved form were detected, similar to wild-type protein (Fig. 3*A*). In contrast, in the L101P, L982P, L1553P, and Q1591P mutant proteins, which were mainly localized at the ER, the amount of the 180-kDa cleaved form was considerably decreased, compared with that of wild-type protein, to an undetectable level (Fig. 3*A*). In the L982P, L1553P, and Q1591P mutant proteins, although the amount of 220-kDa noncleaved-form protein appears increased compared with that of wild-type protein in Fig. 3*A*, the total amount of ABCA3-GFP (220-kDa noncleaved form plus 180-kDa cleaved form) did not differ significantly among seven missense mutant proteins and the wild-type protein ($n = 3$, data not shown). The 4552insT mutation of the *ABCA3* gene in fatal surfactant deficiency (12) causes a frameshift at Gly-1518 and introduces a Trp residue followed by a stop codon, the encoded Ins1518fs mutant protein lacking the C-terminal polypeptide containing the Walker B sequence of NBD-2 (Fig. 1*A*). In the Ins1518fs mutant protein, the level of the cleaved form (expected size of 150 kDa) also was considerably decreased to an undetectable level (Fig. 3*A*).

To examine the processing of oligosaccharides prior to proteolytic cleavage, the total membrane fraction prepared from transiently transfected HEK293 cells was treated with PNGase F or Endo H and analyzed by immunoblotting (Fig. 3, *B* and *C*). Endo H cleaves two proximal *N*-acetylglucosamine residues of the high mannose-type sugar chains but not of the complex-type ones, whereas PNGase F cleaves both types. Treatment with PNGase F increased the electrophoretic mobility of 220-

FIGURE 2. **Subcellular localization of wild-type ABCA3-GFP and mutant proteins in cultured cells.** *A*, *panels a–d*, A549 cells stably expressing wild-type ABCA3-GFP (*panel a*) were grown on glass coverslips and processed for immunofluorescence labeling of LAMP3 (*panel b*), a marker of lamellar bodies and multivesicular bodies. Nuclei were counterstained by 4,6-diamidino-2-phenylindole (*DAPI*) (*c*). A merged image of *panels a–c* is shown in *panel d*. *Panels e–h*, HEK293 cells transiently expressing wild-type ABCA3-GFP (*panel e*) were processed for immunofluorescence labeling of LAMP3 (*panel f*). Nuclei were counterstained by 4,6-diamidino-2-phenylindole (*g*). A merged image of *panels e–g* is shown in *h*. *Panels i–l*, HEK293 cells transiently co-expressing wild-type ABCA3-GFP (*panel i*), DsRed2-ER (*panel j*), and cyan fluorescent protein-Golgi (*panel k*) are shown. A merged image of *panels i–k* is shown in *panel l*. *B*, HEK293 cells transiently expressing mutant ABCA3-GFP proteins (*panels a, d, g,* and *j*) were processed for immunofluorescence labeling of LAMP3 (*panels b, e, h,* and *k*): N568D (*panels a–c*), G1221S (*panels d–f*), L1580P (*panels g–i*), and L101P (*panels j–l*). Merged images are shown in *panels c, f, i,* and *l*. *C*, HEK293 cells transiently co-expressing mutant ABCA3-GFP proteins (*panels a, d, g, j,* and *m*) and DsRed2-ER (*panels b, e, h, k,* and *n*) are shown: L101P (*panels a–c*), L982P (*panels d–f*), L1553P (*panels g–i*), Q1591P (*panels j–l*), and Ins1518fs (*panels m–o*). Merged images are shown in (*panels c, f, i, l,* and *o*). The *scale bar* represents 5 μm.

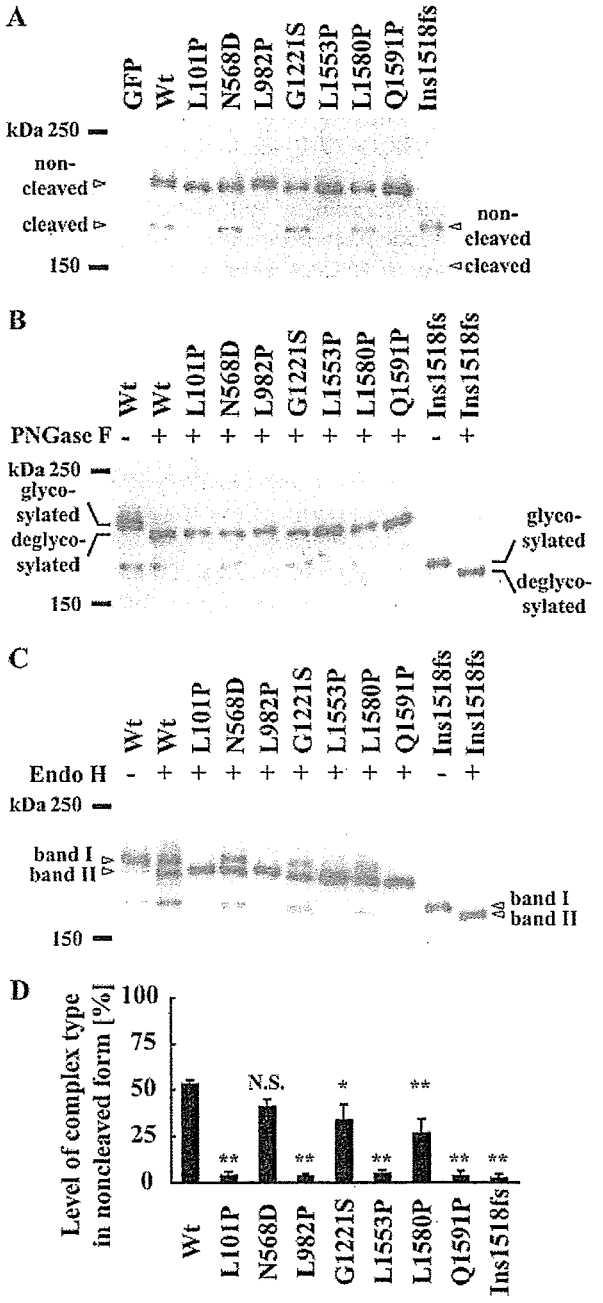


FIGURE 3. **Processing and glycosylation of wild-type ABCA3-GFP and mutant proteins in HEK293 cells.** *A*, 10 $\mu$g of total membrane fractions from HEK293 cells transiently transfected with GFP, wild-type (*Wt*) ABCA3-GFP, or mutants was subjected to SDS-PAGE (5%), transferred to PVDF membranes, and analyzed by using anti-GFP monoclonal antibody. The position of noncleaved 220-kDa ABCA3-GFP protein (wild-type and missense mutants) and 190-kDa protein (nonsense Ins1518fs mutant) is indicated. The position of cleaved 180-kDa ABCA3-GFP proteins (wild-type and missense mutants) and 150-kDa protein (nonsense Ins1518fs mutant) is also indicated. *B*, 10 $\mu$g of total membrane fraction with (+) or without (−) treatment of PNGase F was subjected to SDS-PAGE and immunoblot analysis. ABCA3-GFP proteins modified with oligosaccharide (220 kDa in wild-type and missense mutants and 190 kDa in Ins1518fs) were deglycosylated by PNGase F and produced 210-kDa (wild-type and missense mutant) and 180-kDa (Ins1518fs) proteins. *C*, 10 $\mu$g of total membrane fraction with (+) or without (−) treatment of Endo H was subjected to SDS-PAGE and immunoblot analysis. *Band I* shows Endo H-insensitive 220-kDa ABCA3-GFP proteins (wild-type, N568D, L982P, and L1553P) containing complex-type sugar chains. ABCA3-GFP proteins modified with high mannose-type sugar chains were digested by Endo H and produced 210-kDa (wild-type and missense mutants) and 180-kDa (Ins1518fs) proteins (*band II*). *D*, percentage of ABCA3-GFP protein modified with complex-type sugar chains in noncleaved protein. The amount of each protein was quantified by measuring the density of the band. The level of wild-type and mutant ABCA3-GFP protein in band I (Endo H-insensitive 220-kDa protein except for 190-kDa Ins1518fs protein) is represented as a percentage of total band I plus band II (Endo H-sensitive 210-kDa protein except for 180-kDa Ins1518fs protein). *, $p < 0.05$; **, $p < 0.005$ *versus* wild type. *N.S.*, not significant.

kDa wild-type ABCA3-GFP and the seven missense mutant (L101P, N568D, L982P, G1221S, L1553P, L1580P, and Q1591P) proteins to produce a 210-kDa deglycosylated protein (Fig. 3*B*). Electrophoretic mobility shift from 190 to 180 kDa also was observed in the Ins1518fs nonsense mutant protein (Fig. 3*B*), indicating that all eight mutants are *N*-glycosylated as is wild-type ABCA3-GFP protein.

When the total membrane fraction from cells expressing wild-type ABCA3-GFP was analyzed by Endo H digestion, the amounts of the 220-kDa undigested ABCA3-GFP protein (band I) and of the 210-kDa digested protein (band II) were comparable (Fig. 3*C*). This indicates that about 50% of the noncleaved 220-kDa wild-type ABCA3-GFP protein is modified with complex-type sugar chains that are insensitive to Endo H (Fig. 3, *C* and *D*). In the N568D, G1221S, and L1580P mutant proteins, about 30–40% of the 220-kDa protein remained as Endo H-insensitive complex-type protein (Fig. 3, *C* and *D, band I*), indicating that processing of oligosaccharide from high mannose type to complex type is largely preserved in these mutants. However, in the L101P, L982P, L1553P, Q1591P, and Ins1518fs mutant proteins, the levels of complex-type protein (band I) were dramatically decreased compared with that of wild-type protein (Fig. 3, *C* and *D*). More than 95% of the 220-kDa proteins of the four missense mutants and the 190-kDa protein of the Ins1518fs nonsense mutant was sensitive to Endo H digestion, producing 210- and 180-kDa proteins (band II), respectively, indicating that most of these ABCA3 mutant proteins are modified with high mannose-type sugar chains. These results indicate that the N568D, G1221S, and L1580P mutant proteins are mainly localized at the intracellular vesicle membrane accompanied by processing of oligosaccharide from high mannose type to complex type, whereas the four missense mutant (L101P, L982D, L1553P, and Q1591P) and one nonsense mutant (Ins1518fs) proteins remain localized at the ER, with impaired processing of oligosaccharide.

*ATP Hydrolysis of ABCA3-GFP and Mutants*—To investigate the mechanism of loss of function of the N568D, G1221S, and L1580P mutant proteins that are trafficked to intracellular vesicles accompanied by processing of sugar chains as is wild-type ABCA3 protein, we examined ATP hydrolysis of wild-type ABCA3-GFP and the mutant proteins. ABCA3 protein efficiently traps Mg-ADP in the presence of orthovanadate, an analog of phosphate, and forms a stable inhibitory intermediate during the ATP hydrolysis cycle (26). The intermediate can be specifically photoaffinity-labeled in the membrane after ATP hydrolysis when 8-azido-[$\alpha$-$^{32}$P]ATP is used as an ATP analog.

To examine vanadate-induced nucleotide trapping in ABCA3-GFP and the mutant proteins, HEK293 cells stably

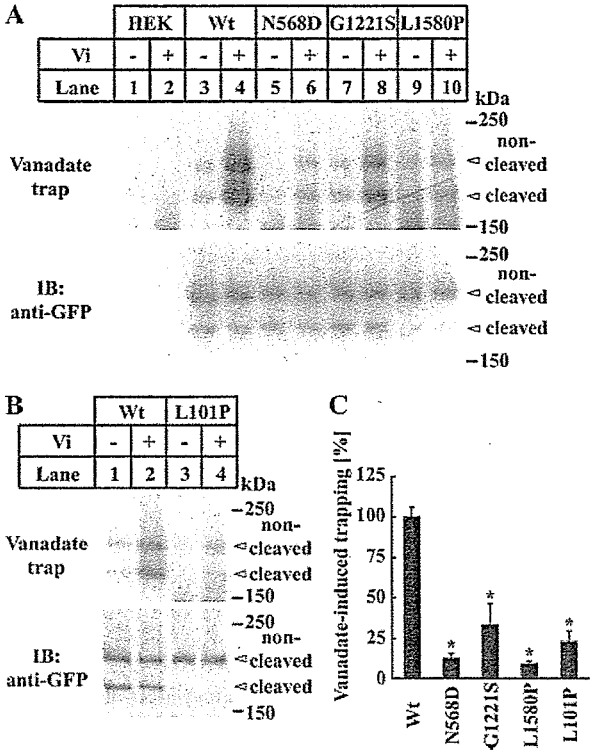


FIGURE 4. **Vanadate-induced nucleotide trapping in ABCA3-GFP and mutant proteins.** *A*, 20,000 × *g* membrane fraction prepared from HEK293 cells stably expressing the wild-type (*Wt*) ABCA3-GFP (*lanes 3* and *4*), N568D (*lanes 5* and *6*), G1221S (*lanes 7* and *8*), L1580P (*lanes 9* and *10*), or untransfected HEK293 cells (*lanes 1* and *2*) was incubated with 10 μM 8-azido-[α-$^{32}$P]ATP in the absence (−) or presence (+) of 0.4 mM orthovanadate (*Vi*) and 3 mM $MgCl_2$ for 10 min at 37 °C. Proteins were photoaffinity-labeled with UV irradiation after removal of unbound ATP, electrophoresed on SDS-PAGE (5%), and transferred to a PVDF membrane. Membrane was analyzed by autoradiography (*upper panel*) and immunoblotting (*IB*) using anti-GFP antibody (*lower panel*). *B*, 20,000 × *g* membrane fraction prepared from HEK293 cells stably expressing the wild-type (*Wt*) ABCA3-GFP (*lanes 1* and *2*) or L101P (*lanes 3* and *4*) was similarly analyzed. *C*, radioactivities of photoaffinity-labeled protein (total 220-kDa noncleaved form plus 180-kDa cleaved form) were quantified by FLA-5000. Radioactivities in the absence of orthovanadate were subtracted from radioactivities in the presence of orthovanadate and are expressed after normalization to ABCA3-GFP protein (total 220-kDa noncleaved form plus 180-kDa cleaved form). Data are represented as means ± S.D. ($n = 4$). *, $p < 0.005$ *versus* wild type.

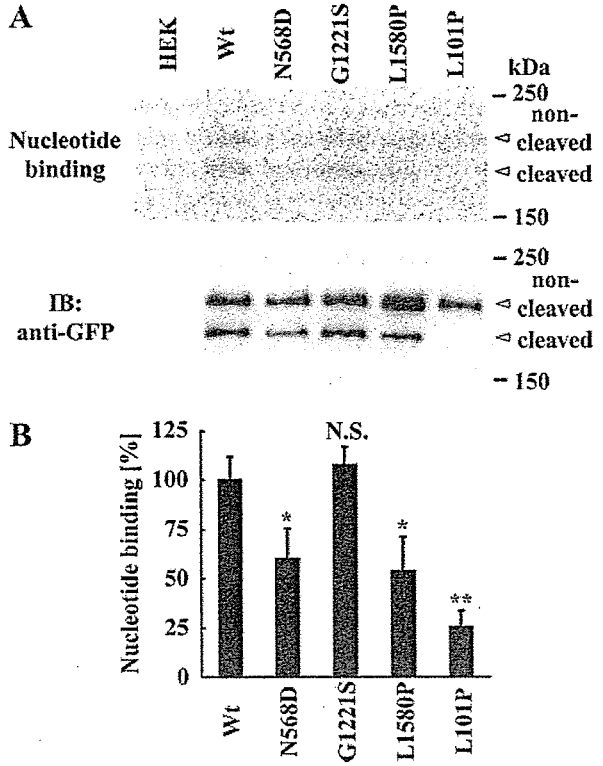


FIGURE 5. **Binding of ABCA3-GFP and mutant proteins with 8-azido-[γ-$^{32}$P]ATP.** *A*, 20,000 × *g* membrane fraction prepared from HEK293 cells stably expressing wild-type (*Wt*) ABCA3-GFP, N568D, G1221S, L101P, or untransfected HEK293 cells was incubated with 20 μM 8-azido-[γ-$^{32}$P]ATP and 3 mM $MgCl_2$ for 10 min at 0 °C. Proteins were photoaffinity-labeled with UV irradiation, immunoprecipitated using anti-human ABCA3 antibody, electrophoresed on SDS-PAGE (5%), and transferred to a PVDF membrane. Membrane was analyzed by BAS-2000 (*upper panel*) and immunoblotting (*IB*) using anti-GFP antibody (*lower panel*). *B*, radioactivities of photoaffinity-labeled protein (total 220-kDa noncleaved form plus 180-kDa cleaved form) were quantified by BAS-2000 and expressed after normalization to ABCA3-GFP protein (total 220-kDa noncleaved form plus 180-kDa cleaved form). Data are represented as means ± S.D. ($n = 3$). *, $p < 0.05$; **, $p < 0.01$ *versus* wild type. *N.S.*, not significant.

expressing wild-type or mutant (N568D, G1221S, and L1580P) ABCA3-GFP fusion proteins were established. In the stably expressing cells, wild-type and the mutant ABCA3-GFP proteins were mainly localized to intracellular vesicle membrane as in transiently expressed cells (data not shown). Among 20,000 × *g* membrane fractions of the cells expressing wild-type ABCA3-GFP, 220-kDa (noncleaved form) and 180-kDa (cleaved form) proteins were slightly photoaffinity-labeled with 8-azido-[α-$^{32}$P]ATP in the absence of orthovanadate (Fig. 4*A*, *lane 3*), and photoaffinity labeling was induced in the presence of orthovanadate (Fig. 4*A*, *lane 4*). Although we used ABCA3-GFP fusion protein in this study, these results are consistent with our previous observation using ABCA3 without GFP fusion (26). In the N568D, G1221S, and L1580P mutant proteins, vanadate-induced nucleotide trapping was significantly decreased to 12, 33, and 9% of that of the wild-type protein, respectively (Fig. 4, *A*, *lanes 5–10*, and *C*). These results indicate that ATP hydrolysis activity is severely impaired in these mutants.

To examine ATP hydrolysis of the mutant retained to the ER, cells stably expressing L101P mutant protein were established. L101P mutant protein was mainly localized to the ER, consistent with the result in transiently expressing cells (data not shown). The vanadate-induced nucleotide trapping also was significantly decreased compared with that of wild-type protein (Fig. 4*B*, *lanes 3* and *4*), indicating that ATP hydrolysis activity as well as intracellular trafficking is impaired in the L101P mutant protein.

*ATP Binding of ABCA3-GFP and Mutants*—To clarify the mechanism of loss of ATP hydrolysis activity of the N568D, G1221S, and L1580P mutant proteins, we examined ATP binding of wild-type ABCA3-GFP and the mutant proteins. Among the 20,000 × *g* membrane fractions of the cells expressing wild-type ABCA3-GFP, the 220-kDa (noncleaved form) and the 180-kDa (cleaved form) proteins were photoaffinity-labeled with 8-azido-[γ-$^{32}$P]ATP (Fig. 5*A*). The membrane fraction of the untransfected HEK293 cells was not photoaffinity-labeled. The level of photoaffinity labeling of the G1221S mutant protein

with 8-azido-[$\gamma$-$^{32}$P]ATP was similar to that of wild-type ABCA3-GFP protein (Fig. 5, *A* and *B*). However, the levels of photoaffinity labeling of N568D and L1580P mutant proteins were moderately decreased to 60 and 54% of that of wild-type protein, respectively. The level of photoaffinity labeling of L101P protein remaining localized at the ER was considerably decreased to 25% that of wild-type protein. These results suggest that decreased ATP binding contributes to impaired ATP hydrolysis in the N568D, L1580P, and L101P mutants but not in the G1221S mutant.

*ATP Hydrolysis of Site-directed Mutants of Gly-1221 in 11th Transmembrane Segment*—Since transmembrane domains and NBDs are suggested to communicate during the ATP hydrolysis cycle (31), local environmental changes in the 11th transmembrane segment (TM-11) resulting from the G1221S mutation might allosterically impair ATP hydrolysis activity of the ABCA3 protein. To address this, the effects of introducing hydroxyl groups or alteration of side-chain size on ATP hydrolysis activity were investigated by generating three site-directed mutants (G1221A, G1221V, and G1221T), which were stably expressed in HEK293 cells. These mutant proteins were mainly localized to intracellular vesicle membrane (data not shown). In the G1221T mutant protein, which had hydroxyl-containing amino acids, vanadate-induced nucleotide trapping was decreased to 36% of that of wild-type protein, as also in G1221S mutant protein (Fig. 6, *A*, *lanes 9–12*, and *B*). In the G1221A and G1221V mutant proteins, which have a hydrophobic side chain, vanadate-induced nucleotide trapping was decreased to 15 and 18% of that of wild-type protein, respectively (Fig. 6, *A*, *lanes 5–8*, and *B*). This result indicates the significance of the small side chain of Gly-1221 (H atom) in TM-11 for ATP hydrolysis.

*ATP Hydrolysis of Site-directed Mutants of Leu-1580 in NBD-2*—Because both leucine and proline are hydrophobic amino acids, alteration of side-chain size could be responsible for the impaired ATP hydrolysis in the L1580P mutant. Accordingly, Leu-1580 was substituted with three hydrophobic amino acids, Ala, Val, and Phe, of different size. All three mutant proteins were stably expressed in HEK293 cells and were mainly localized to intracellular vesicle membrane (data not shown). Substitution with Val, the side chain of which is smaller than that of Leu, resulted in decreased vanadate-induced nucleotide trapping of 56% that of wild-type protein (Fig. 7, *A*, *lanes 7* and *8*, and *B*). Substitution with Ala, the side chain of which is much smaller than that of Val, resulted in decreased vanadate-induced nucleotide trapping of 13% that of wild-type protein (Fig. 7, *A*, *lanes 5* and *6*, and *B*). On the other hand, substitution with Phe, the side chain of which is larger than that of Leu, also caused a dramatic decrease in vanadate-induced nucleotide trapping to 13% that of wild-type protein (Fig. 7, *A*, *lanes 9* and *10*, and *B*). These results indicate that appropriate side-chain size of Leu-1580 at NBD-2 is important for ATP hydrolysis of ABCA3.

*Homology Modeling of NBD-2 of ABCA3*—The relationship between side-chain size and ATP hydrolysis activity of Leu-1580 mutant proteins suggests side-chain contact of Leu-1580 with other amino acids in the ABCA3 protein. To address this question, the secondary structures of NBD of ABCA3 and other

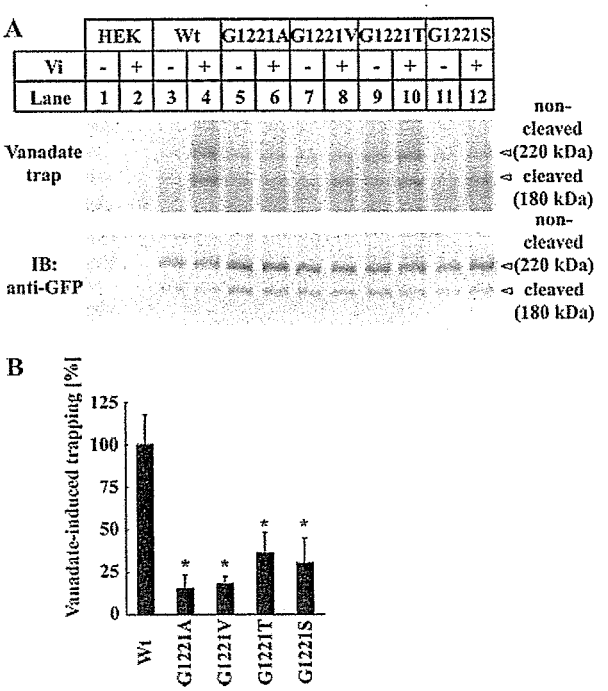


FIGURE 6. **Vanadate-induced nucleotide trapping in site-directed mutant proteins of Gly-1221.** *A*, 20,000 × *g* membrane fraction prepared from HEK293 cells stably expressing wild-type (*Wt*) ABCA3-GFP (*lanes 3* and *4*), G1221A (*lanes 5* and *6*), G1221V (*lanes 7* and *8*), G1221T (*lanes 9* and *10*), G1221S (*lanes 11* and *12*), or untransfected HEK293 cells (*lanes 1* and *2*) was incubated with 10 $\mu$M 8-azido-[$\alpha$-$^{32}$P]ATP in the absence (−) or presence (+) of 0.4 mM orthovanadate (*Vi*) and 3 mM $MgCl_2$ for 10 min at 37 °C. Proteins were photoaffinity-labeled with UV irradiation after removal of unbound ATP, electrophoresed on SDS-PAGE (5%), and transferred to a PVDF membrane. Membrane was analyzed by autoradiography (*upper panel*) and immunoblotting (*IB*) using anti-GFP antibody (*lower panel*). *B*, radioactivities of photoaffinity-labeled protein (total 220-kDa noncleaved form plus 180-kDa cleaved form) were quantified by FLA-5000. Radioactivities in the absence of orthovanadate were subtracted from radioactivities in the presence of orthovanadate and are expressed after normalization to ABCA3-GFP protein (total 220-kDa noncleaved form plus 180-kDa cleaved form). Data are represented as means ± S.D. ($n$ = 4–5). *, $p < 0.01$ *versus* wild type.

ABC transporters were first predicted (32) and compared with that of *Escherichia coli* maltose transporter MalK (Fig. 8*A*), of which the crystal structure has been solved (33). Leu-1580 was predicted to locate at helix 7 (referred from the study of vitamin B transporter BtuD; Ref. 34) adjacent to the H-loop His residue, which is well conserved and known to form a strong hydrogen bond with the $\gamma$-phosphate of ATP. We then modeled the structure of NBD-2 of ABCA3 based on the ATP-bound closed form of MalK (Protein Data Bank entry 1Q12; Ref. 33) using SWISS-MODEL (35). In the model of ABCA3, the orientations of His-1572 and Leu-1580 in ABCA3 were similar to those of His-192 and Leu-200 in MalK, respectively (Fig. 8, *B* and *C*). In the model of ABCA3, Trp-1554 is the most proximal residue from Leu-1580 in amino acids located at helix 6, and the distance from $\delta$-carbon of Leu-1580 to $\beta$-carbon of Trp-1554 (the nearest carbon) was ~4.4 Å, which is close to van der Waals contact. In MalK, the distance from $\delta$-carbon of Leu-200 to $\beta$-carbon of corresponding Arg-173 at helix 6 was ~4.2 Å, comparable with the calculated distance in ABCA3. Substitution of Leu-1580 with Pro, considering the best rotamer conformation, extended the distance from $\gamma$-carbon of Pro-1580 to $\beta$-carbon of Trp-1554 to 5.4 Å (Fig. 8*D*). In the L1580V mutant protein,

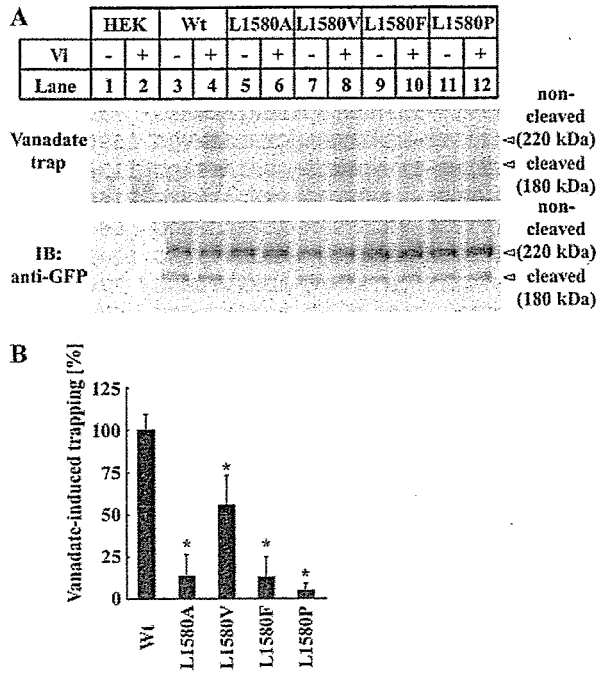


FIGURE 7. **Vanadate-induced nucleotide trapping in site-directed mutant proteins of Leu-1580.** *A*, 20,000 × *g* membrane fraction prepared from HEK293 cells stably expressing wild-type (*Wt*) ABCA3-GFP (*lanes 3* and *4*), L1580A (*lanes 5* and *6*), L1580V (*lanes 7* and *8*), L1580F (*lanes 9* and *10*), L1580P (*lanes 11* and *12*), or untransfected HEK293 cells (*lanes 1* and *2*) was incubated with 10 μM 8-azido-[α-$^{32}$P]ATP in the absence (−) or presence (+) of 0.4 mM orthovanadate (*Vi*) and 3 mM $MgCl_2$ for 10 min at 37 °C. Proteins were photoaffinity-labeled with UV irradiation after removal of unbound ATP, electrophoresed on SDS-PAGE (5%), and transferred to a PVDF membrane. Membrane was analyzed by autoradiography (*upper panel*) and immunoblotting (*IB*) using anti-GFP antibody (*lower panel*). *B*, radioactivities of photoaffinity-labeled protein (total 220-kDa noncleaved form plus 180-kDa cleaved form) were quantified by FLA-5000. Radioactivities in the absence of orthovanadate were subtracted from radioactivities in the presence of orthovanadate and are expressed after normalization to ABCA3-GFP protein (total 220-kDa noncleaved form plus 180-kDa cleaved form). Data are represented as means ± S.D. ($n = 3–4$). *, $p < 0.01$ *versus* wild type.

which had moderately impaired ATP hydrolysis, the distance from γ-carbon of Val-1580 to β-carbon of Trp-1554 was calculated as 4.9 Å (Fig. 8*F*). In the L1580A and L1580F mutant proteins, which had dramatically impaired ATP hydrolysis, the distance from β-carbon of Ala-1580 and ζ-carbon of Phe-1580 was extended to 6.3 Å and shortened to 2.2 Å, respectively, compared with that of wild-type protein (Fig. 8, *E* and *G*). These biochemical and modeling analyses suggest that an appropriate distance between Trp-1554 at helix 6 and 1580th amino acid at helix 7 in NBD-2 is important for ATP hydrolysis of the ABCA3 protein. Thus, impaired ATP hydrolysis in the L1580P mutant protein may result in part from the alteration of side-chain size.

## DISCUSSION

Pulmonary surfactant, composed mainly of phospholipids and specific surfactant proteins, reduces the surface tension at the alveolar air-liquid interface, thereby preventing the lungs from collapsing. However, the mechanisms of surfactant production in alveolar type II cells and secretion into the alveolar space are unknown. Recently, mutations in the *ABCA3* gene were found in newborns with fatal surfactant deficiency (12). In this study, we examined the intracellular localization and *N*-glycosylation of eight ABCA3 mutant proteins, most of the mutations found in fatal surfactant deficiency to date. In addition, we examined ATP hydrolysis and ATP binding activities of the representative mutants.

Investigating the intracellular localization and *N*-glycosylation of these ABCA3 mutant proteins in HEK293 cells, we found the missense L101P, L982P, L1553P, Q1591P, and nonsense Ins1518fs mutant proteins to be predominantly localized at the ER, with impaired processing of oligosaccharide. W1142*X* mutant ABCA3 protein, another nonsense mutant reported in fatal surfactant deficiency (12), also was predominantly localized at the ER with impaired processing of oligosaccharide (data not shown).

Some mutations of ABC transporters associated with human disease have been reported to induce intracellular mislocalization of the protein. For example, R587W and Q597R mutations of ABCA1, which are found in Tangier disease patients with high density lipoprotein deficiency, appear to be impaired in intracellular trafficking and localized predominantly to the ER (36). One amino acid (Phe-508) deletion of the cystic fibrosis transmembrane conductance regulator (CFTR) hampers trafficking of protein from the ER to the plasma membrane (37), and proper folding of the CFTR protein is thought to be essential for the coat complex II-dependent export of the protein from the ER (38). Interestingly, a single amino acid is substituted with a proline residue in the four mutant ABCA3 proteins (L101P, L982P, L1553P, and Q1591P) that are retained at the ER. As three of these mutations (L101P, L982P, and L1553P) are located in the predicted α-helical structure of the ABCA3 protein (32) and the proline residue is known to be helix breaker (39), its introduction into the ABCA3 protein might well disrupt the α-helical structure and hamper proper folding and intracellular translocation. The large C-terminal deletion of the ABCA3 protein (Ins1518fs and W1142*X*) also might hamper this process. Indeed, patients with homozygous mutations of L101P, L1553P, and W1142*X* have been reported to die of surfactant deficiency during the neonatal period, and electron microscopic study of lung tissue from patients with homozygous L1553P and W1142*X* mutations revealed smaller lamellar bodies than those in normal lung tissue (12). These observations suggest that trafficking of ABCA3 protein from the ER to the intracellular LAMP3-positive vesicle is essential not only for the function of the ABCA3 protein but also for the maturation of lamellar bodies and alveolar surfactant metabolism.

In contrast, the N568D, G1221S, and L1580P mutant proteins were localized to intracellular vesicle membrane accompanied by processing of oligosaccharide from high mannose type to complex type as found in wild-type ABCA3 protein. However, vanadate-induced nucleotide trapping analysis revealed ATP hydrolysis activity to be significantly decreased in N568D, G1221S, and L1580P mutant ABCA3 proteins compared with wild type. Thus, the mechanism of surfactant deficiency because of *ABCA3* gene mutation can be classified into two categories as follows: abnormal intracellular trafficking (type I) and decreased ATP hydrolysis activity with normal intracellular trafficking (type II). Although patients with

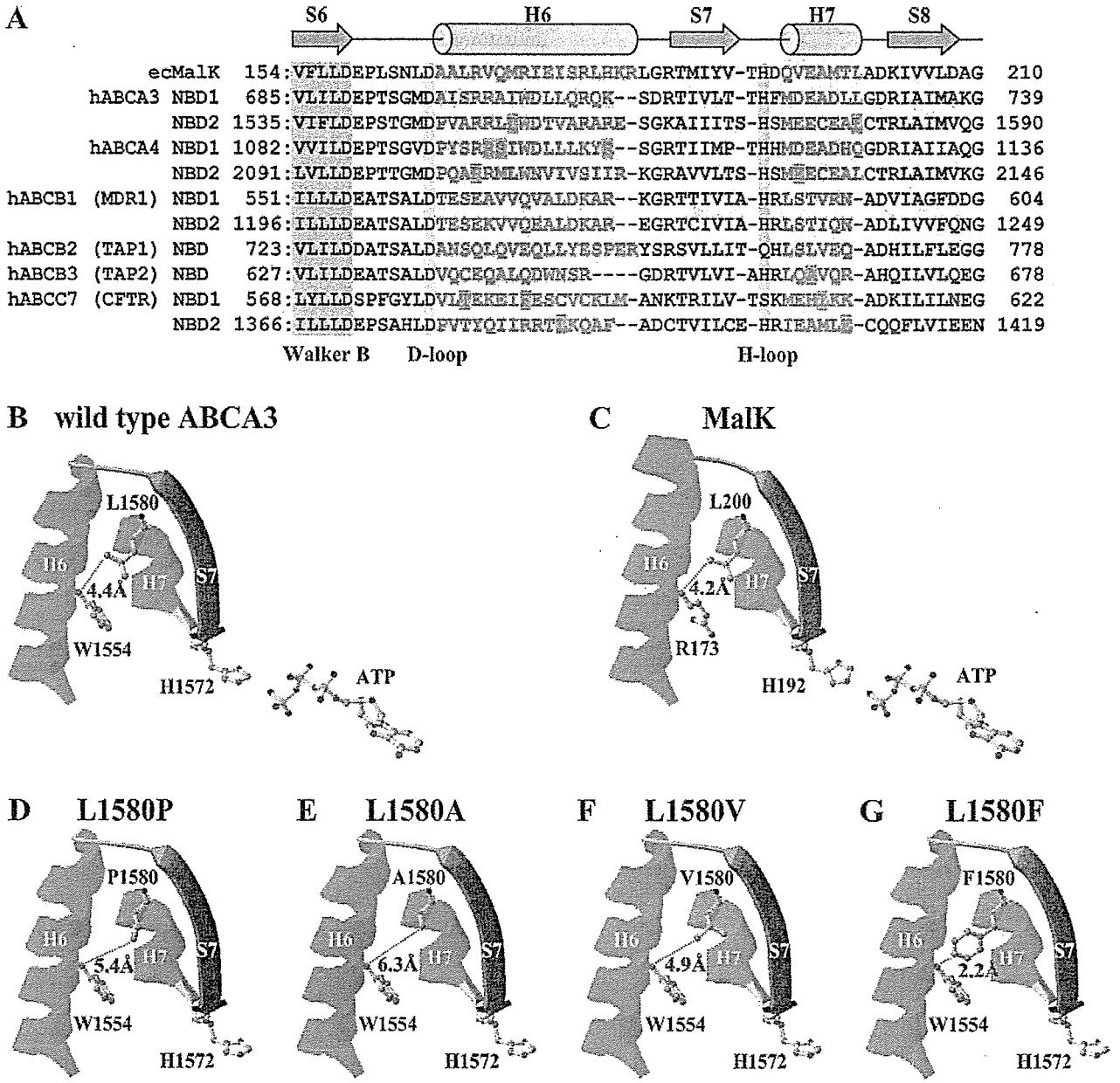


FIGURE 8. **Multiple alignment of partial NBD sequences of ABC transporters and homology modeling of NBD-2 of ABCA3.** *A*, secondary structures of NBD of human ABCA3 and other ABC transporters were predicted, and partial amino acid sequences of NBD were aligned based on the predicted secondary structures. Amino acids predicted to form α-helix, β-sheet, and coil are shown in *green*, *red*, and *black*, respectively, and compared with that of *E. coli* maltose transporter ecMalK. Critical conserved sequence motifs (Walker B, D-loop, and H-loop) are highlighted. Secondary structure elements are indicated *above* the sequence. The number of helix and sheet was referred from the study of vitamin B transporter BtuD (34). Amino acids associated with disease at helices 6 and 7 are highlighted with *yellow*. *B–G*, model structure of NBD-2 of ABCA3 (*B*) based on the ATP-bound closed form of MalK (*C*) using SWISS-MODEL is shown. For clarity, only the region from helix 6 to helix 7 is shown. The models of mutant L1580P (*D*), L1580A (*E*), L1580V (*F*), and L1580F (*G*) ABCA3 proteins were generated from that of wild-type protein by choosing the best rotamer conformation of the mutant amino acid. The 1580th residue (Leu-200 in the case of MalK) at helix 7, H-loop His residue, Trp-1554 residue (Arg-173 in the case of MalK) at helix 6, and ATP are indicated. *H*, α-helix; *S*, β-sheet.

homozygous type II *ABCA3* mutations have not been reported, patients with type I/type II compound heterozygous *ABCA3* mutations (L982P/G1221S and Ins1518fs/L1580P) died of surfactant deficiency during the neonatal period, and the lamellar bodies of lung tissue from a patient with L982P/G1221S were reported to be smaller than those from normal lung tissue (12). Because type I *ABCA3* mutation on one allele does not result in fatal surfactant deficiency, these results suggest that a sufficient level of ATP hydrolysis activity of the ABCA3 protein encoded in the other allele is essential for the function of the ABCA3 protein, maturation of the lamellar bodies, and surfactant metabolism.

Type II mutations lie in various locations as follows: N568D in the Walker A motif of NBD-1, G1221S in TM-11, and L1580P in NBD-2 (Fig. 1*A*), and all of these amino acids are conserved in the ABCA subfamily (Fig. 1, *B–D*). Because Asn-568 is highly conserved in the Walker A motif and is thought to be critical for the binding of γ-phosphate of ATP, as predicted

from the crystal structure of other ABC transporters (40), both ATP binding and ATP hydrolysis activities should be impaired in the N568D mutant protein.

It has been reported that some mutations in transmembrane domains of ABC transporters affect the activity of NBDs. For example, the E1204L mutation in TM-16 of MRP1(multidrug resistance associated protein 1) affects vanadate-induced nucleotide trapping as well as transport activity of the protein (41). In this study, mutational analysis of Gly-1221 in ABCA3 has shown the significance of the side chain of the Gly residue (H atom) in TM-11 for ATP hydrolysis. In membrane proteins, Gly is found at twice the frequency than in soluble proteins, and it is suggested that the small side chain of Gly is important for tight helix packing and helix-helix association of membrane proteins in the lipid bilayer (42). Because conserved Gly residues were found in TM-5, TM-6, TM-10, TM-11, and TM-12 of the ABCA subfamily, and also in TMs of other subfamilies such as TM-17 in the ABCC subfamily (43), these Gly residues may well contribute to the geometry of TMs that is important for communication between transmembrane domains and NBDs.

Mutational analysis of Leu-1580 suggested that impaired ATP hydrolysis in the L1580P mutant protein is in part due to the change in side-chain size. However, because Pro is known as a helix breaker (39), disruption of helix 7 by the introduction of the Pro residue may also contribute to the impaired ATP hydrolysis in the case of the L1580P mutant protein. Homology modeling of NBD-2 of ABCA3 showed that the distance between 1580th amino acid at helix 7 and Trp-1554 at helix 6 of NBD-2 is related to ATP hydrolysis of the ABCA3 protein. Because helix 7 was adjacent to the H-loop His residue, it is possible that helix 7 interacts with helix 6 to maintain the orientation of His for efficient hydrogen bonding with the γ-phosphate of ATP. Although further confirmation of this interaction might be provided by mutational analysis of Trp-1554, many disease-related mutations at helix 6 and helix 7 of NBDs such as R2106C and E2131K in ABCA4 (44–47), F587I and L610S in ABCC7/CFTR (48–50), and A665T in ABCB3/TAP2 (51) (Fig. 8*A*) support the importance of these helices for the function of the ABC transporter.

In this study, the 180-kDa cleaved protein in stably transfected cells appears to be higher in wild-type than in transiently transfected cells (Figs. 3–5). Indeed, the former is about 20–45% and the latter is about 10–20% of total 220-kDa noncleaved form plus the 180-kDa cleaved form, using total membrane fractions (data not shown). In addition, the level of vanadate-induced nucleotide trapping of the 180-kDa cleaved form protein is approximately two times higher than that of the 220-kDa noncleaved form protein after normalization to the protein level (Fig. 4*A*, *lanes 3* and *4*). Because cleaved protein is predominantly expressed in native lung tissue (21, 23), the processing of ABCA3 protein from noncleaved form to cleaved form may be physiologically important in ABCA3 function. Further studies are needed to understand the structure-function relationships of the ABCA3 protein.

We examined ATP binding and ATP hydrolysis of the type I mutant ABCA3 protein by using cells stably expressing L101P mutant protein, and we found that both ATP binding and ATP hydrolysis activities as well as intracellular trafficking were impaired in the L101P mutant protein. Although we did not examine ATP binding and ATP hydrolysis of other type I mutants, these results indicate that intracellular trafficking and also ATP binding and ATP hydrolysis activities are impaired in some type I mutant ABCA3 proteins.

Thus, intracellular trafficking and/or activity of ATP hydrolysis is dramatically impaired in the ABCA3 mutant proteins so far found in fatal surfactant deficiency patients. Such ABCA3 protein dysfunction could well underlie the severe phenotype of these patients. Very recently, it has been reported that the E292V mutation of the *ABCA3* gene is responsible in the genetic etiology of pediatric interstitial lung disease related to abnormal surfactant function (24), the phenotype of which is milder than that of fatal surfactant deficiency. It is possible that the E292V mutation causes less severe disruption of intracellular trafficking or ATP hydrolysis activity. Additional biochemical studies are required to clarify the loss of function mechanisms for the mutations associated with milder pediatric interstitial lung disease.

Very recently, Cheong *et al.* (19) reported that L101P, G1221S, and N568D mutant proteins have the most severe, moderate, and the least severe trafficking and processing defects. In this study, the difference in degree of defect between N568D and G1221S mutant proteins is slight, if any. The reason for the difference between their results and ours is unknown, but it may be due to the different clonal cells used stably expressing ABCA3 mutants. With regard to the function of the ABCA3 mutant proteins, their findings indicating impaired colocalization of fluorescence-labeled phosphatidylcholine with ABCA3-positive vesicles in G1221S and N568D may well correlate with our findings indicating impaired ATP hydrolysis activities of these mutants.

In summary, the mechanisms of surfactant deficiency because of *ABCA3* gene mutation can be classified into two categories, type I and type II, abnormal intracellular trafficking and decreased ATP hydrolysis activity. This distinction may be useful in assessing both the severity and effective therapy for lung disease because of mutation of the *ABCA3* gene.

*Acknowledgments—We thank Drs. Jun-ichi Miyazaki (Osaka University) and Hitoshi Niwa (RIKEN, Kobe) for providing the pCAGIpuro plasmid.*

## REFERENCES

1. Rooney, S. A. (2001) *Comp. Biochem. Physiol.* **129,** 233–243
2. Mason, R. J., and Voelker, D. R. (1998) *Biochim. Biophys. Acta* **1408,** 226–240
3. Chander, A., and Fisher, A. B. (1990) *Am. J. Physiol.* **258,** L241–L253
4. Wright, J. R., and Dobbs, L. G. (1991) *Annu. Rev. Physiol.* **53,** 395–414
5. Dobbs, L. G. (1994) *Am. J. Respir. Crit. Care Med.* **150,** S31–S32
6. Batenburg, J. J., and Whitsett, J. A. (1989) *Biochim. Biophys. Acta* **1006,** 329–334
7. Zimmermann, L. J., Hogan, M., Carlson, K. S., Smith, B. T., and Post, M. (1993) *Am. J. Physiol.* **264,** L575–L580
8. Beneke, S., and Rooney, S. A. (2001) *Biochim. Biophys. Acta* **1534,** 56–63
9. Liley, H. G., White, R. T., Warr, R. G., Benson, B. J., Hawgood, S., and Ballard, P. L. (1989) *J. Clin. Investig.* **83,** 1191–1197